

Predicting a Decadal Shift in North Atlantic Climate Variability Using the GFDL Forecast System

RYM MSADEK,* T. L. DELWORTH,⁺ A. ROSATI,⁺ W. ANDERSON,⁺ G. VECCHI,⁺ Y.-S. CHANG,*[#]
K. DIXON,⁺ R. G. GUDGEL,⁺ W. STERN,⁺ A. WITTENBERG,⁺ X. YANG,* F. ZENG,⁺
R. ZHANG,⁺ AND S. ZHANG⁺

* NOAA/GFDL, Princeton, New Jersey, and UCAR, Boulder, Colorado

⁺ NOAA/GFDL, Princeton, New Jersey

(Manuscript received 31 July 2013, in final form 4 June 2014)

ABSTRACT

Decadal prediction experiments were conducted as part of phase 5 of the Coupled Model Intercomparison Project (CMIP5) using the GFDL Climate Model, version 2.1 (CM2.1) forecast system. The abrupt warming of the North Atlantic Subpolar Gyre (SPG) that was observed in the mid-1990s is considered as a case study to evaluate forecast capabilities and better understand the reasons for the observed changes. Initializing the CM2.1 coupled system produces high skill in retrospectively predicting the mid-1990s shift, which is not captured by the uninitialized forecasts. All the hindcasts initialized in the early 1990s show a warming of the SPG; however, only the ensemble-mean hindcasts initialized in 1995 and 1996 are able to reproduce the observed abrupt warming and the associated decrease and contraction of the SPG. Examination of the physical mechanisms responsible for the successful retrospective predictions indicates that initializing the ocean is key to predicting the mid-1990s warming. The successful initialized forecasts show an increased Atlantic meridional overturning circulation and North Atlantic Current transport, which drive an increased advection of warm saline subtropical waters northward, leading to a westward shift of the subpolar front and, subsequently, a warming and spindown of the SPG. Significant seasonal climate impacts are predicted as the SPG warms, including a reduced sea ice concentration over the Arctic, an enhanced warming over the central United States during summer and fall, and a northward shift of the mean ITCZ. These climate anomalies are similar to those observed during a warm phase of the Atlantic multidecadal oscillation, which is encouraging for future predictions of North Atlantic climate.

1. Introduction

The increased demand for short-term climate projections on spatial scales that are relevant for societal applications has spurred considerable research in the field of decadal climate prediction. Decadal climate variations arise as the result of externally forced and natural fluctuations, both of which are potential sources of predictability. The attempt to predict the externally forced climate change signal has motivated the numerous experiments performed in support of the Intergovernmental

Panel on Climate Change (IPCC) since the early 1990s. In these experiments, coupled climate models were forced with historical and projected changes in external forcing (e.g., greenhouse gases, aerosols, and volcanoes) with the goal of projecting future climate changes and understanding their mechanisms in response to this forcing. These experiments did not explicitly attempt to predict the additional component of climate change that arises from natural variability, as such predictions required initializing the climate models with observations (Meehl et al. 2009). The ocean, with its large-scale inertia and its low-frequency variations, has long been considered an integrator of high-frequency atmospheric fluctuations (Frankignoul and Hasselmann 1977), thus providing memory and a potential source of predictability to the whole climate system (Griffies and Bryan 1997). Regions where natural variability is large with respect to forced changes have been highlighted as regions of high potential predictability (Boer 2004, 2011). These

[#] Current affiliation: Kongju National University, Gongju, South Korea.

Corresponding author address: Rym Msadek, NOAA/GFDL, 201 Forrestal Road, Princeton, NJ 08540.
E-mail: rym.msadek@noaa.gov

include the North Atlantic, North Pacific, and Southern Oceans.

Initial studies carried out by individual models have shown promising improvements arising from initializing the ocean (Smith et al. 2007; Keenlyside et al. 2008). This motivated the recent phase 5 of the Coupled Model Intercomparison Project (CMIP5) coordinated decadal prediction experiments, in which a number of climate models were initialized using observed estimates, with the goal of predicting some oceanic-driven internal variability as well as externally forced changes (Mehta et al. 2011; Taylor et al. 2012). A number of studies have already documented the results of these experiments, showing globally modest additional skill arising from initialization (Mochizuki et al. 2012; van Oldenborgh et al. 2012; Doblas-Reyes et al. 2011; Garcia-Serrano et al. 2012; Goddard et al. 2013; Meehl et al. 2014). In most regions, large correlations arise from predicting the long-term trend, which is largest in the Indian Ocean (Guemas et al. 2013). Some skill in predicting natural fluctuations in the North Pacific has also been outlined in some models (Mochizuki et al. 2010), but the robustness of these results remains uncertain. The North Atlantic, in contrast, stands out as a region where correlations are improved also because of initial conditions (Yang et al. 2013; Hazeleger et al. 2013; Wouters et al. 2013; Meehl et al. 2014) with, in particular, some skill in predicting variations associated with the Atlantic multidecadal sea surface temperature variability (AMV). A multimodel analysis, part of the Ensemble-Based Predictions of Climate Changes and their Impacts (ENSEMBLES) project, indicates that the improved skill in AMV likely results from initializing the North Atlantic Subpolar Gyre (SPG), whereas the overall AMV skill is being degraded by the limited skill in predicting Atlantic variations in the subtropics (Garcia-Serrano et al. 2012). This is consistent with a number of studies that point to the North Atlantic SPG as a region where internal variability is the main driver of decadal fluctuations (Lozier et al. 2008; Ting et al. 2009; Terray 2012).

A strong warming of the North Atlantic SPG was observed in the mid-1990s, with surface temperatures increasing by more than 1°C in less than five years (Robson et al. 2012a). Observations also reveal a weakening and a westward contraction of the SPG as the North Atlantic Oscillation (NAO) switched from a positive to a negative phase in the mid-1990s (Bersch 2002; Flatau et al. 2003; Häkkinen and Rhines 2004; Bersch 2007; Lozier et al. 2008). Abrupt changes in northeastern Atlantic marine ecosystems have been observed following the decline and change of shape of the SPG (Hátún et al. 2005, 2009). Predicting such a climatic event even a few years in advance would be of high

interest for fishing activities in the area (Keyl and Wolff 2008; Stock et al. 2011). Two hypotheses are discussed in Robson et al. (2012a) for the mid-1990s warming that we also consider in the present study. First, it has been suggested that internal multidecadal variability was a possible driver of this decline (Böning et al. 2006), with little influence from external forcing, which is consistent with the lack of abrupt SPG changes in the coupled simulations forced by increased greenhouse gases (Yeager et al. 2012; Robson et al. 2012b). A change in weather regimes (Cassou et al. 2004), like the shift from a positive to a negative phase of the NAO that occurred during the winter 1995/96, was also suggested to be a possible driver of these oceanic changes, either directly through air–sea fluxes or as a lagged response through variations in the oceanic circulation (Lohmann et al. 2009a,b). Indeed, winters during which the NAO index is positive are known to be associated with increased westerlies across the SPG, resulting in larger heat loss in the ocean, an increase in the gyre strength, and an eastward shift of the subpolar front (Curry and McCartney 2001; Hurrell 2003; Visbeck et al. 2003; Hátún et al. 2005; Yashayaev 2007). However, repeated years of positive NAO favor convective activity and deep-water formation in the Labrador Sea, which can, in turn, enhance the Atlantic meridional overturning circulation (AMOC). A stronger AMOC is associated with a larger transport of heat from the subtropics northward in the Atlantic (Johns et al. 2011; Msadek et al. 2013). Therefore, a sustained positive NAO could have driven a shift from an anomalously cold to an anomalously warm SPG through dynamical oceanic changes, as shown by Lohmann et al. (2009a) and Robson et al. (2012a). Such a mechanism, if true, would mean that changes like those associated with the 1995 warming would be predictable, if the ocean state after a sustained positive NAO is imposed and the modeled AMOC correctly responds to it. Another hypothesis for the observed warming is the abrupt change of phase of the NAO during the winter of 1995/96, from a positive to a highly negative NAO, the latter being associated with an anomalously warm SPG. In this scenario, the North Atlantic abrupt warming would be an instantaneous response to atmospheric changes and, hence, because of the limited predictability of atmospheric variability beyond a few days, the event would not be predictable in our decadal experiments.

Recent studies by Lohmann et al. (2009a,b) and Robson et al. (2012a) support the first hypothesis rather than the latter. Robson et al. (2012a) suggested that the unusually negative NAO index that occurred during the winter of 1995/96 might have contributed to the rapidity of the warming but was unlikely to be the fundamental cause. The predictive skill of this North Atlantic abrupt

warming event has been investigated by [Robson et al. \(2012b\)](#) and [Yeager et al. \(2012\)](#) in the Met Office decadal prediction system (DePreSys) and the National Center for Atmospheric Research (NCAR) Community Climate System Model, version 4 (CCSM4) decadal prediction experiments, respectively. In both studies, a warming of the SPG appeared in some of the retrospective predictions, referred to as hindcasts, initialized in the early 1990s, albeit at a slower rate than observed, which was explained in terms of a lack of skill to predict the NAO itself. The predicted warming was attributed to the enhanced meridional heat transport (MHT) associated with the intensified AMOC following the initialization. [Yeager et al. \(2012\)](#) argued that any of their forecasts initialized between 1990 and 1995 would have predicted the same warming, suggesting that the ocean preconditioning was strong enough in the early 1990s to drive the warming. However they did not test this hypothesis, as only one experiment was conducted in the 1990s with a start date prior to the SPG warming (1991). CMIP5 recommended that decadal predictions be conducted every year to test the sensitivity to the oceanic initial state. The predictions in [Robson et al. \(2012b\)](#) were initialized every year, and the largest warming was found in the 1994 DePreSys forecasts. The predictions of the SPG warming described by [Yeager et al. \(2012\)](#) and [Robson et al. \(2012b\)](#) show many similarities in terms of mechanisms, including the key role of the AMOC in driving the northward advection of warm waters. However, some differences can be outlined between these two studies, which to our knowledge are the only two that investigated in detail the predictive skill of the mid-1990s SPG warming. In the DePreSys experiments, the shift was due to a convergence of heat in the SPG, whereas in CCSM4, it was interpreted, from a budget analysis, as an imbalance between strong advection of heat and surface heat flux cooling when the NAO changed sign.

Salinity variations can impact the upper-ocean density, the rate of deep-water formation and hence the strength of the AMOC. [Hazeleger et al. \(2013\)](#) found that North Atlantic surface salinity was highly predictable in the Thermohaline Overturning-at Risk? (THOR) multimodel ensemble but skill was more limited and more difficult to assess for depth-integrated salinity. The role of salinity in the success of the mid-1990s SPG warming predictions was not explored by [Yeager et al. \(2012\)](#) and [Robson et al. \(2012b\)](#).

Although the mid-1990s warming of the North Atlantic has been shown to be predictable a few years ahead in the previous two studies, it is important to assess whether this feature is robust across other prediction systems. One would expect the magnitude and timing of the North Atlantic predicted warming to

depend on the model used to run the predictions, as well as on the ocean initialization and details of the assimilation scheme ([Bellucci et al. 2013](#)). Coupled models show a large range in the mechanisms driving the fluctuations of the AMOC on decadal time scales ([Msadek and Frankignoul 2009](#); [Frankcombe et al. 2010](#); [Kwon and Frankignoul 2012](#); [Escudier et al. 2013](#); [Sévellec and Fedorov 2013](#)). The timing of the shift in the predictions will therefore likely depend on the adjustment response of the simulated AMOC to NAO forcing ([Eden and Willebrand 2001](#); [Deshayes and Frankignoul 2008](#)).

Significant climate impacts have been identified in several coupled models in response to natural fluctuations of the AMOC ([Knight et al. 2006](#); [Msadek et al. 2011](#)), with anomalies that are comparable to those driven by the AMV in observations ([Sutton and Hodson 2005](#); [Zhang and Delworth 2006](#)). [Robson et al. \(2013\)](#) compared the DePreSys hindcasts initialized before and after the mid-1990s warming and identified significant seasonal impacts over North America, western Europe, and the tropical Atlantic region, with some similarities to observations. Natural variations of the AMOC and the AMV in a long control simulation of the Geophysical Fluid Dynamics Laboratory's (GFDL) Climate Model, version 2.1 (CM2.1) have also been linked to observed changes in temperature and sea ice in the Arctic region ([Mahajan et al. 2011](#)). This suggests that North Atlantic changes like the SPG mid-1990s warming could have impacted Arctic variability, a link that has not been investigated in previous predictability studies.

In this paper, we analyze the predictive skill of the mid-1990s North Atlantic SPG warming using the GFDL CM2.1 forecast system. Unlike other CMIP5 predictions, our forecast system is initialized using balanced initial conditions from the Ensemble Coupled Data Assimilation (ECDA) ([Zhang et al. 2007](#); [Chang et al. 2013](#)) with start dates every year. The model and experiments that are used in this analysis are described in [section 2](#). Results of the initialized predictions of the mid-1990s SPG changes are presented in [section 3](#), followed by a description of the proposed mechanism that operates in the GFDL CM2.1 initialized predictions ([section 4](#)). Significant climate anomalies over the Arctic and North Atlantic regions are found in the predictions that successfully capture the abrupt warming, as presented in [section 5](#). Discussion and conclusions are given in [section 6](#).

2. Description of the forecast model and experiments

a. Design of the decadal prediction experiments

The GFDL decadal prediction experiments are based on the GFDL CM2.1 ([Delworth et al. 2006](#)) and are

initialized using the ECDA (Zhang et al. 2007; Chang et al. 2013). ECDA is based on an ensemble adjustment Kalman filter (Anderson 2001) applied to the fully coupled climate model CM2.1 (Zhang et al. 2007), which ensures a better-balanced initialization than if each component of the climate system were using its own assimilation system. Both atmospheric and oceanic components are constrained by observations using a full-field assimilation. The atmosphere is constrained by the NCEP atmospheric analysis (Kalnay et al. 1996) and the ocean assimilates observations of SST from satellite [optimum interpolation SST (OISST)] and temperature and salinity from the World Ocean Database 2009 (Boyer et al. 2009), which includes profiles from expendable bathythermograph temperature (XBT) and Argo profiles after year 2000. Systematic biases associated with the fall rate of XBT are corrected following the method of Hanawa et al. (1995) and Kizu et al. (2005), as described in more detail in Chang et al. (2013). Because salinity data are sparser than temperature data, ECDA uses pseudosalinity obtained from the temperature–salinity (T – S) relationship, using XBT data down to 500–700 m and altimetry information (Chang et al. 2011a,b). The altimetry sea surface height (SSH) information is partially used for the generation of pseudosalinity profiles (Chang et al. 2011a,b) but is not directly assimilated to the current ECDA system. ECDA includes Argo profiles since their advent in the early 2000s, which provide observations of the global ocean over the upper 2000 m (Roemmich and Gilson 2009), offering the potential to initialize ocean heat and density anomalies.

Ten-member ensembles are initialized on 1 January of every year between 1961 and 2012 and run for 10 years (giving a total of 5200 model years). The ensemble size of ECDA is 12. We focus on annual means in this paper; hence, year 1 (or lead 1 yr) of the prediction corresponds to the January–December mean following the initialization. For 1961–2005, the model is forced with observationally based estimates of changing concentrations of greenhouse gases and aerosols, land use changes, solar irradiance variations, and volcanic aerosols. After 2005, the model is forced with estimates of changing greenhouse gases and aerosols based on the representative concentration pathways (RCP4.5) scenario (Meinshausen et al. 2011). In addition to these 10-member initialized predictions, we run a 10-member ensemble of uninitialized retrospective predictions (also referred to as projections or forced experiments) using the same model and the same radiative forcing as in the initialized experiments but with no information about the observed initial state. These simulations are intended to provide the forced response of the climate system and are compared to the initialized predictions to determine the impact of initialization.

The global skill of these GFDL decadal prediction experiments has been investigated in a companion paper by Yang et al. (2013). Most of the decadal skill of CM2.1 in SST and ocean heat content (OHC) arises from the climate response to radiative forcing with overall little impact of initialization except in the North Atlantic and Southern Oceans (Yang et al. 2013), which is in agreement with other CMIP5 model experiments (Kim et al. 2012; Garcia-Serrano et al. 2012; Goddard et al. 2013; Hazeleger et al. 2013). Yang et al. (2013) further showed that the most predictable pattern on decadal time scales in the Atlantic projects on a structure that resembles the observed Atlantic multidecadal oscillation (AMO) or AMV pattern. Encouraging results for predicting tropical Atlantic variations and, in particular, North Atlantic hurricane frequency were also found in the CM2.1 decadal prediction experiments (Vecchi et al. 2013). Here, we use the same forecast suite to investigate the skill in predicting the North Atlantic SPG warming that occurred in the mid-1990s.

b. Lead-dependent climatology

While there are various ways to initialize climate predictions, we can briefly describe two main procedures that are most commonly used: the full-field initialization and the anomaly initialization. Full-field initialization brings the model state close to observations and, as a consequence, the model then drifts toward its own mean state, requiring the predictions to be bias adjusted (Kumar et al. 2012; Goddard et al. 2013; Meehl et al. 2014). Anomaly initialization adds the anomalous component of the observed state to the model climatology, thereby minimizing the drift during the prediction. However, it produces mismatches between the observational anomalies and the model climatology without fully eliminating the drift (Robson 2010). The GFDL CM2.1 predictions use a full-field assimilation, which tends to be favored by most modeling groups (Smith et al. 2013), although a more systematic evaluation would be needed to draw firm conclusions on which technique is best and whether it has an impact on predictive skill. Following the protocol suggested for CMIP5 (ICPO 2011), we take the model's systematic error into account by removing, from each forecast, a lead-dependent climatology. We build a climatology that depends on lead time by averaging, for each lead time between 1 and 10 years, the forecasts that verify in the years 1986–2005. For example, a 1995 annual mean anomaly predicted at a 1-yr (2-yr) lead has been initialized in January 1995 (1994), so the anomaly is defined by subtracting from the first (second) year of the prediction the 1986–2005 mean value predicted at the 1-yr (2-yr) lead. The model climatology is computed by averaging all 10 ensemble members. The

key impact of subtracting the lead-dependent climatology is to remove the systematic bias that arises in the forecasts as the model drifts toward its own mean state (Stockdale 1997). By defining a fixed climatology (1986–2005), we make the assumption that the model drift does not depend on the initialization period: that is, the systematic drift does not depend on the changes to the climate observing system that have occurred in the last 50 years. This is quite a strong assumption that could affect the assessment of forecast skill (Kumar et al. 2012; Vecchi et al. 2013).

3. Results

a. Forecast skill assessment for North Atlantic OHC changes in the mid-1990s

Prior to 1995, the North Atlantic upper-ocean temperatures were characterized by cold anomalies in the SPG with respect to the 1961–90 mean and warm anomalies in the subtropics (Fig. 1a). This dipolar pattern turned into a uniform warming across the whole North Atlantic basin after 1995, a warming that persisted for more than a decade. The abrupt warming of the North Atlantic upper ocean and the associated decline of the SPG strength in the mid-1990s are quite well reproduced in ECDA. This is expected, as observed surface and subsurface temperatures have been assimilated. Overall, as shown by Chang et al. (2013), the mean and variability of upper-ocean heat content compare well with other observational analyses (Levitus et al. 2005; Ingleby and Huddleston 2007; Levitus et al. 2009). We will therefore use the ECDA reanalysis as our observational reference for North Atlantic upper-ocean temperature and salinity and for the SPG strength index (Fig. 1). Hereafter, we will refer to ocean heat content as the potential temperature ($^{\circ}\text{C}$), averaged over the upper 600 m (the actual bottom cell boundary is 617 m, given that we extract the depth level closest to 600 m with no further interpolation). There is a thickening of Labrador Sea mixed layer depth in ECDA between 1991 and 1995 as the NAO persists in its positive phase (not shown). As a result, the SPG displays a gradual strengthening from 1970 onward, and then it strongly declines after 1995 as the NAO reverses (Figs. 1b,c).

The mid-1990s warming of the SPG is retrospectively well predicted by the 5-yr mean and 9-yr mean ensemble-mean initialized predictions compared to the uninitialized ones, although the predicted magnitude is smaller than observed (Fig. 2). This results in a high correlation skill in predicting SPG OHC anomalies (Fig. 3). The SPG OHC time series is defined by the OHC averaged over the region (50° – 65°N , 60° – 10°W) shown by a black box in Fig. 1a. The correlations reach

0.89 at lead 2–6 and remain significant at the 95% level up to lead 5–9 for the 5-yr mean and 2–10 for the 9-yr mean (Fig. 3a). Significance is lost at lead 6–10, as we are further from initial conditions, but it remains statistically significant at the 90% level. The corresponding correlations for the uninitialized predictions are all negative, indicating a lack of skill (Fig. 3a). As some of the skill in the initialized predictions likely arises from the persistence of oceanic anomalies, a persistence forecast is defined as a reference for each lead time. For example, the persistence forecast for lead 2–6 is defined by averaging the observed values over the 5 years that precede the model's initialization. Large correlations are found for the persistence forecast at all lead times, which is consistent with the finding of Branstator et al. (2012) that the memory of the initial state of OHC could persist for about a decade in the GFDL CM2.1 model.

In contrast, the uninitialized predictions show a decline of SPG OHC anomalies starting in the mid-1990s, along with a decline of salinity, a reduced AMOC, and a weakening of the SPG (Fig. 4). The initial AMOC decrease reduces the transport of warm and salty water northward. The lack of salty water in the SPG reduces density, which inhibits deep convection, further weakening the AMOC and the North Atlantic Current (NAC) transport (not shown). The uninitialized experiments therefore show no skill in reproducing the SPG OHC fluctuations during the late twentieth century, suggesting that changes in external forcing were not the primary driver of the observed warming in the mid-1990s. A decrease of the AMOC was also found in the uninitialized DePreSys experiments (Robson et al. 2012b), but it happened in phase with a slow warming of the SPG. This behavior (a warming of the SPG despite an AMOC weakening) is also found in other CMIP5 uninitialized experiments (Cheng et al. 2013), suggesting that while the AMOC response to external forcing might be quite robust, the SPG heat content response is not. The SPG response to external forcing in CM2.1 is also different from the response of the whole North Atlantic basin, which, unlike the SPG, warms in the uninitialized predictions (not shown). This indicates that caution should be taken when attributing observed changes in the whole North Atlantic basin to one single mechanism, as a basin average can hide complex gyre-scale processes (Lozier et al. 2008; Williams et al. 2014). In particular, area-averaged temperature anomalies like the AMV SST index can hide different gyre-scale processes that have different predictive skill (Garcia-Serrano et al. 2012; Terray 2012).

While initialization clearly improves skill in the SPG compared to the uninitialized projections, the large error bars associated with the correlations limit our ability

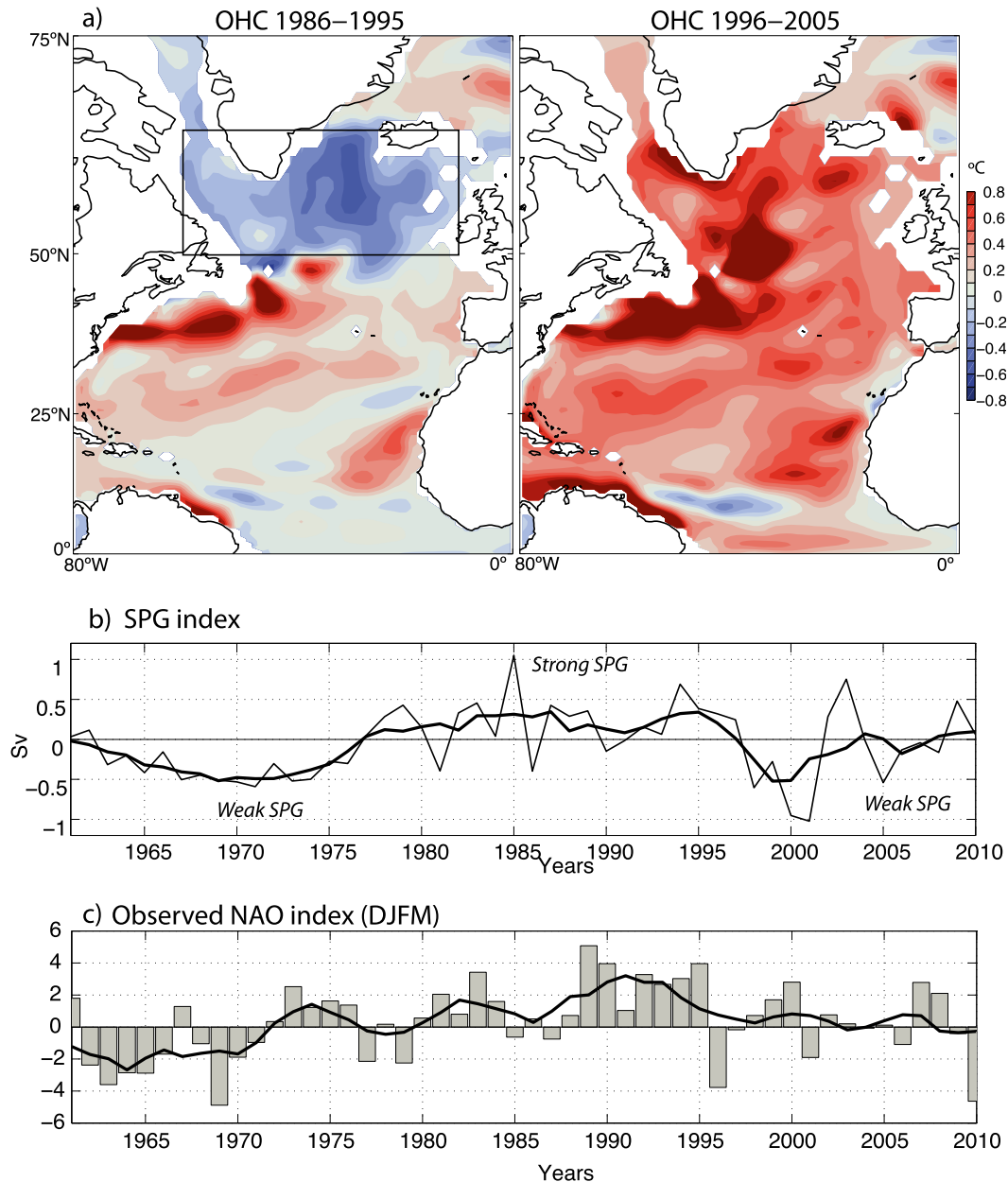


FIG. 1. (a) OHC anomalies ($^{\circ}\text{C}$) estimated from the ECDA observational estimate, averaged over the top 617 m of the ocean: (left) the 1986–95 anomalies with respect to the 1961–90 mean; (right) as in (left), but for the 1996–2005 anomalies. (b) Strength of the SPG in ECDA in sverdrups ($1\text{ Sv} = 10^6\text{ m}^3\text{ s}^{-1}$) defined by the maximum barotropic streamfunction anomalies (with respect to the 1986–2005 climatology) averaged over the subpolar region [50° – 65°N , 60° – 10°W ; black box in (a)]. The index has been inverted so that positive values indicate a stronger gyre. The thin line denotes annual mean values; the thick line is the 5-yr running mean. (c) Observed December–March (DJFM) NAO station-based index from the NCAR Climate Analysis Section (Hurrell 1995).

to assess the significant improvement arising from initialization compared to a simple persistence forecast. This is due to the small number of effective degrees of freedom that results from the short observational record and the highly autocorrelated variables (Vecchi et al. 2013; Hazeleger et al. 2013; Wouters et al. 2013). The

largest difference between the initialized and persistence forecast is found for the second pentad (lead 6–10), suggesting that skill over that lead time cannot be simply attributed to the persistence of initial anomalies. We hypothesize that the large correlations at long lead times also result from the hindcasts' ability to capture the

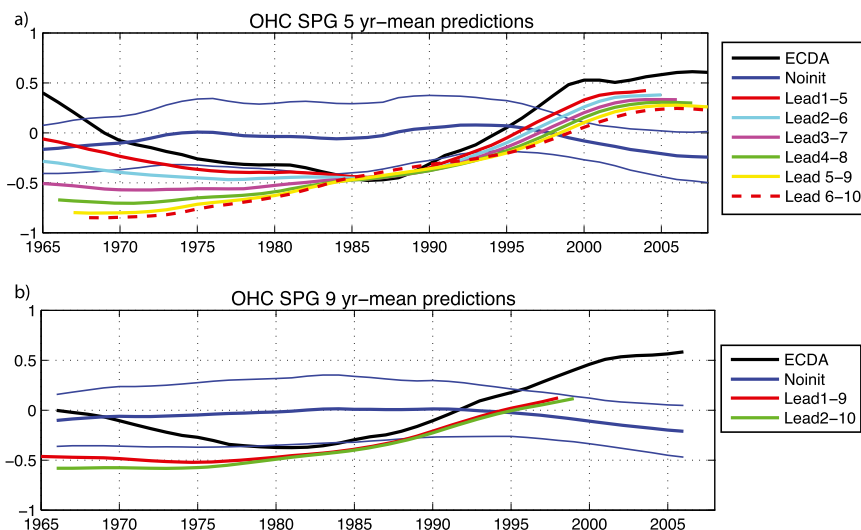


FIG. 2. Time series of the (a) 5-yr mean and (b) 9-yr mean ensemble-mean initialized hindcasts of the SPG OHC anomalies ($^{\circ}\text{C}$) compared with the ECDA observational estimate (black) and the uninitialized predictions (blue). Thin blue lines show the spread of the uninitialized predictions, defined by the standard deviation of the 10 members.

mid-1990s temperature increase, which cannot be captured by a persistence forecast model, and hence motivates the use of a dynamical model.

Following recommendations by [Goddard et al. \(2013\)](#), we use another measure of skill to assess the accuracy of the forecasts, the mean-square skill score (MSSS). The

MSSS is a function of both the correlation and the conditional bias ([Murphy 1988](#)) and it indicates whether a better skill comes from an increased correlation, a reduced conditional bias, or both ([Goddard et al. 2013](#)). We define in Eq. (1) the MSSS as a function of the mean-square error (MSE) between the initialized forecast

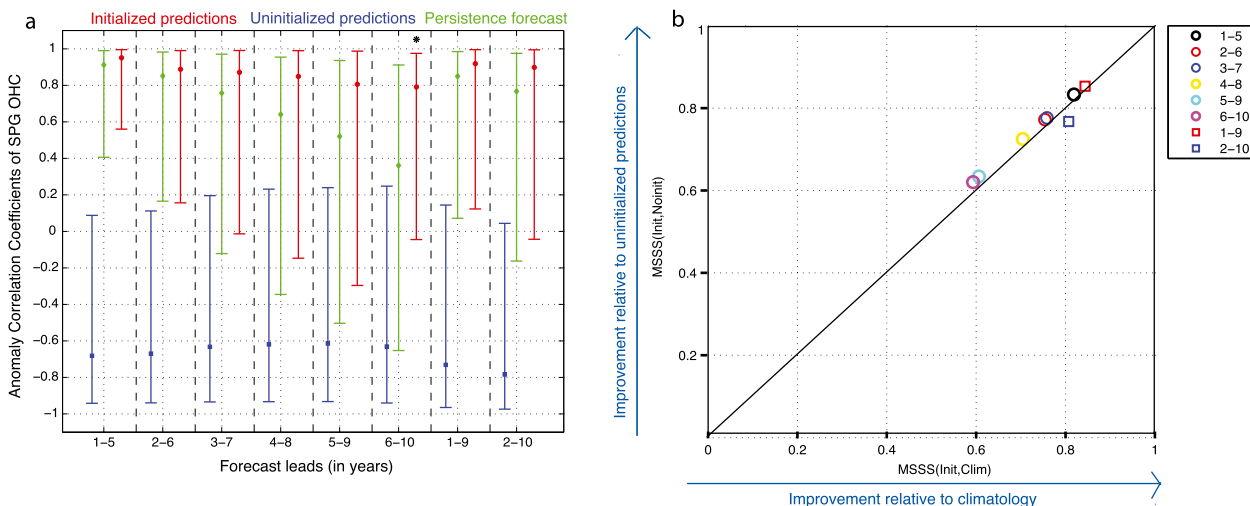


FIG. 3. (a) Anomaly correlations of the North Atlantic SPG OHC anomalies as a function of forecast lead time in the initialized (red), uninitialized (blue), and persistence-based (green) forecasts. The correlation value is shown by a circle, and the bar indicates the two-sided 90% confidence interval of that correlation estimate, defined using Fisher's z transform ([von Storch and Zwiers 1999](#), p. 148). An asterisk on top of a correlation indicates that it is not statistically different from zero at $p = 0.05$ in a single-sided t test. The effective number of degrees of freedom is estimated accounting for serial autocorrelation ([Bretherton et al. 1999](#)). (b) Mean-square skill score of the initialized predictions of SPG OHC anomalies. Positive values on the x (y) axis indicate an increased skill, relative to the forecast climatology (uninitialized predictions). Values indicate the different averaged lead times in years. More details about MSSS computation are given in the text.

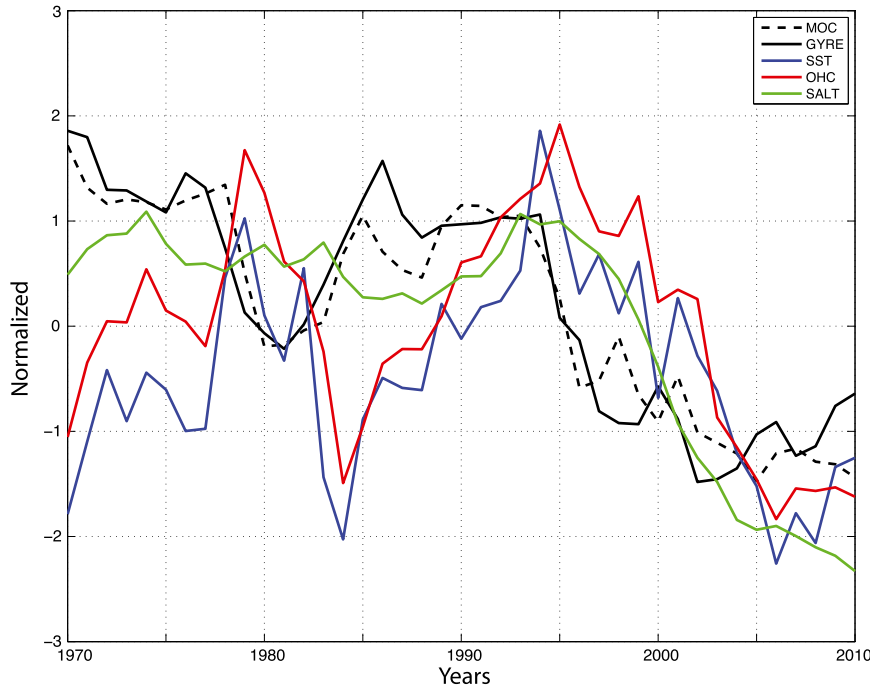


FIG. 4. Time evolution of the AMOC index at 50°N (Sv), the SPG strength index (defined as in Fig. 1, Sv), the SPG SST (°C), the SPG OHC (°C), and the SPG SALT anomalies (psu) in the forced uninitialized experiments. Each time series has been normalized by its standard deviation, and its mean has been removed to facilitate the comparison.

(referred to by the subscript F) and a reference forecast (\bar{X}), as in Vecchi et al. (2013). The reference forecast can be the observed climatology if one wants to evaluate the improvement over climatology, or the uninitialized forecasts if we test the improvement due to initialization. Both are shown in Fig. 3b for the initialized predictions of SPG OHC at different lead times. MSSS is defined as follows:

$$\text{MSSS}(t) = 1 - \frac{\text{MSE}_F(t)}{\text{MSE}_{\bar{X}}(t)}. \quad (1)$$

Positive values of MSSS on the x (y) axis indicate an improvement of skill relative to climatology (uninitialized forecasts) with a maximum value of 1 for perfect accuracy. While values of MSSS decrease as lead time increases, all the values remain positive at all lead times and lie along the one-to-one line, which indicates an improvement with respect to both uninitialized forecasts and climatology. Decomposing further the MSSS indicates that the improvement of accuracy when predictions are started from the observed state results from both a larger correlation and a reduced conditional bias compared to uninitialized forecasts (not shown). Initialization therefore limits the error growth associated with the tendency of the model to evolve toward its own mean

state, as was shown by the multimodel study of Goddard et al. (2013).

b. Sensitivity to initial conditions

The predicted 10-yr trend of SPG OHC anomalies is shown in Fig. 5 for all the hindcasts initialized between 1991 and 1996. All indicate a warming over the prediction period, but the trend is smaller than observed for all except the 1995 and 1996 start dates. The magnitude of the SPG OHC predicted over the first year of 1995 and 1996 hindcasts is smaller than observed, but the trend is comparable to observations (Fig. 5a). The success of the 1995 and 1996 retrospective predictions compared to the other start dates is also illustrated in Fig. 5b, which shows the predicted trend as a function of the observed trend. As the trend is always positive between 1991 and 2000 in observations, positive (negative) values on the y axis indicate the right (wrong) sign in the predicted decadal trend. The values for the uninitialized hindcasts are all negative, consistent with the lack of skill described in Figs. 2 and 3. The hindcasts initialized between 1991 and 1997 all show a consistent sign compared with observations, with too-small values between 1991 and 1994, a perfect agreement in 1995, and a slightly too-large value in 1996. The predicted trend remains positive for the 1997 start date but goes below zero after

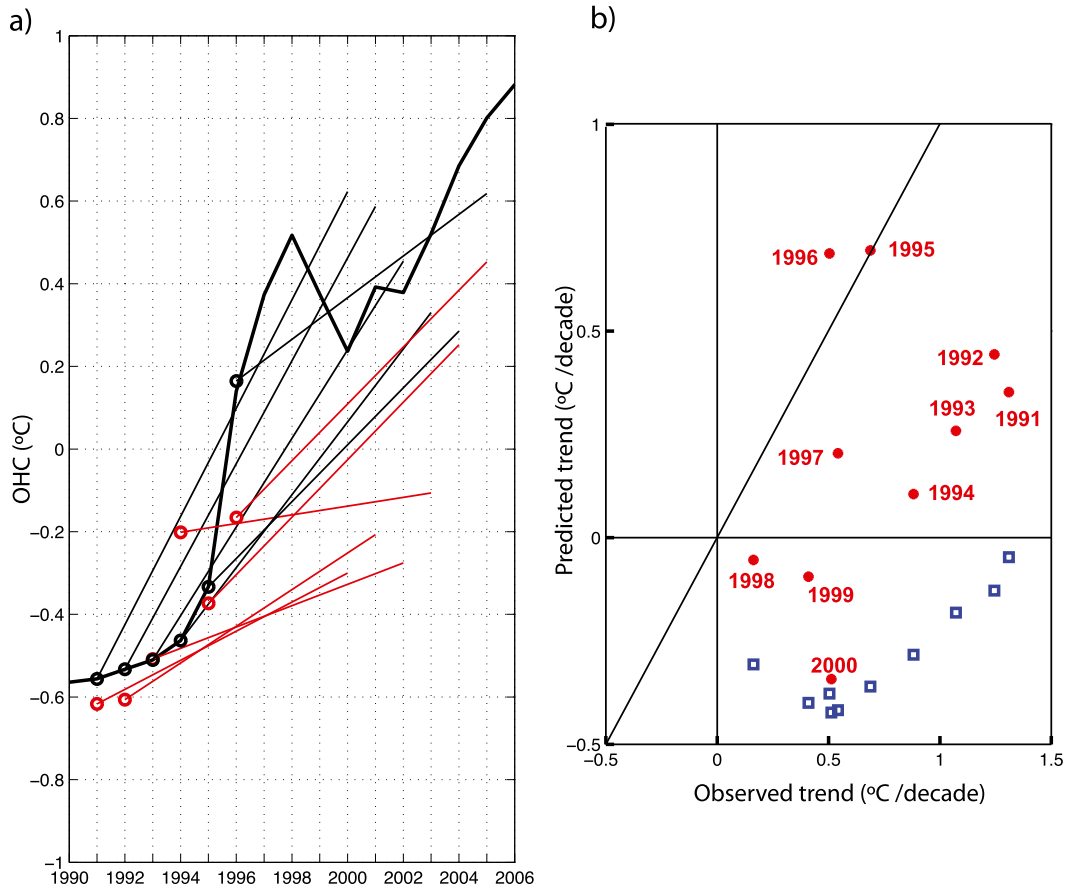


FIG. 5. (a) Observed (black) and ensemble-mean predicted (red) 10-yr trends of SPG OHC anomalies in the hindcasts initialized between 1991 and 1996. (b) Scatterplot of the predicted trend values (y axis) as a function of the observed ones (x axis). The hindcasts initialized between 1991 and 2000 are shown as red dots and are labeled with their start dates. The corresponding values for the uninitialized predictions are shown as blue unlabeled squares.

1998, indicating that skill is lost for the predictions initialized in the late 1990s. This suggests that, although the warming trend persisted in the 2000s, the mechanism was different from that in the mid-1990s or the observing system changed or the assimilation and forecast model failed at reproducing the observed changes.

We next look at the time evolution of the individual hindcasts started between 1991 and 1996 (instead of averaging over a given lead time as in Fig. 2) to determine whether the observed abrupt changes in the SPG strength after 1995 would have been predicted prior to the shift. The ensemble-mean SPG OHC hindcasts, initialized in 1992, warm during the first few years following initialization but much more slowly and with a weaker magnitude than observed (Fig. 6). The mean trajectory of the SPG SST is very similar, indicating comparable skill at the surface and subsurface. The hindcasts initialized in 1991 and 1993 are very similar to those started in 1992 and are therefore not shown here.

The SPG SST and OHC hindcasts initialized in 1994 do not show any warming. Looking at the individual members spread indicates that some members predict a cooling and others a warming (Fig. 7) while, for the other start dates, the spread of the ensemble is as large, but it shows a monotonic warming.

In contrast, the mean hindcasts initialized in 1995 and 1996 warm rapidly, both at the surface and over the upper 600 m. The ensemble mean of the 1995 hindcasts lies near the observations for much of the hindcast period, and the warming occurs at a slightly slower rate than observed, reaching a smaller magnitude than observed at the end of the hindcast period. The 1996 ensemble-mean hindcasts warm more slowly than observed and thus underestimate the magnitude of the warming before 1999. Overall, the ensemble-mean initialized forecasts tend to underestimate the SPG OHC anomalies, as seen in Fig. 2. The 1995 hindcasts envelope does not include the observed trajectory for the first few years, but looking at the individual members indicates

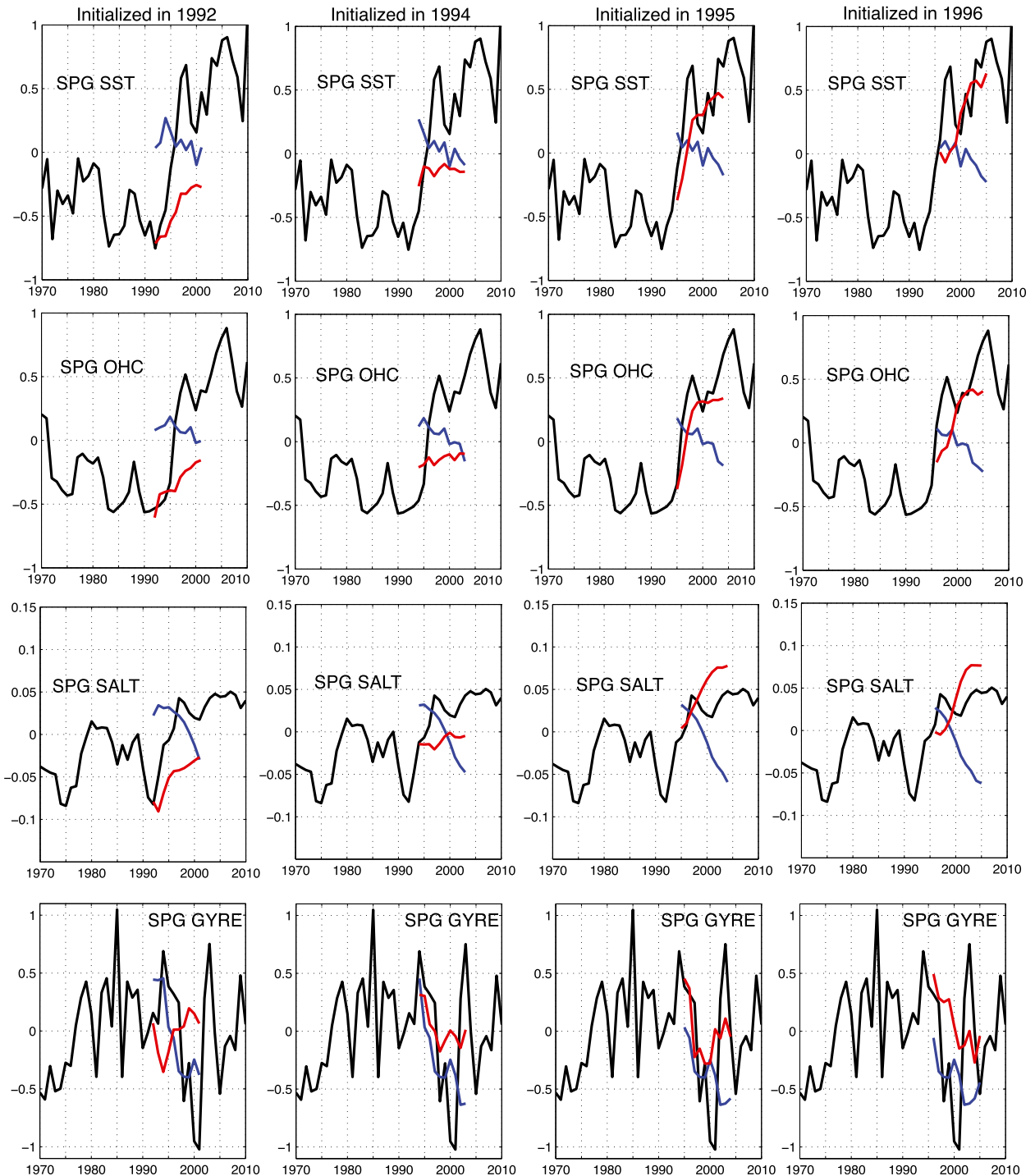


FIG. 6. Ensemble-mean predicted trajectories of North Atlantic SPG OHC anomalies ($^{\circ}\text{C}$), SALT anomalies (psu), and gyre strength anomalies (Sv, defined as in Fig. 1) initialized between 1992 and 1996. Red lines indicate the initialized predictions, blue lines indicate the uninitialized predictions, and the black lines indicate the observed value estimated from ECDA.

that some are able to reproduce both the magnitude and timing of the warming after the 1995 initialization, suggesting that the skill of individual members can exceed that of the ensemble mean (Fig. 7).

Salinity variations in the SPG are less certain than temperature variations because of the sparser observations. The available station data in the SPG indicate marked decadal variability with a large freshening between

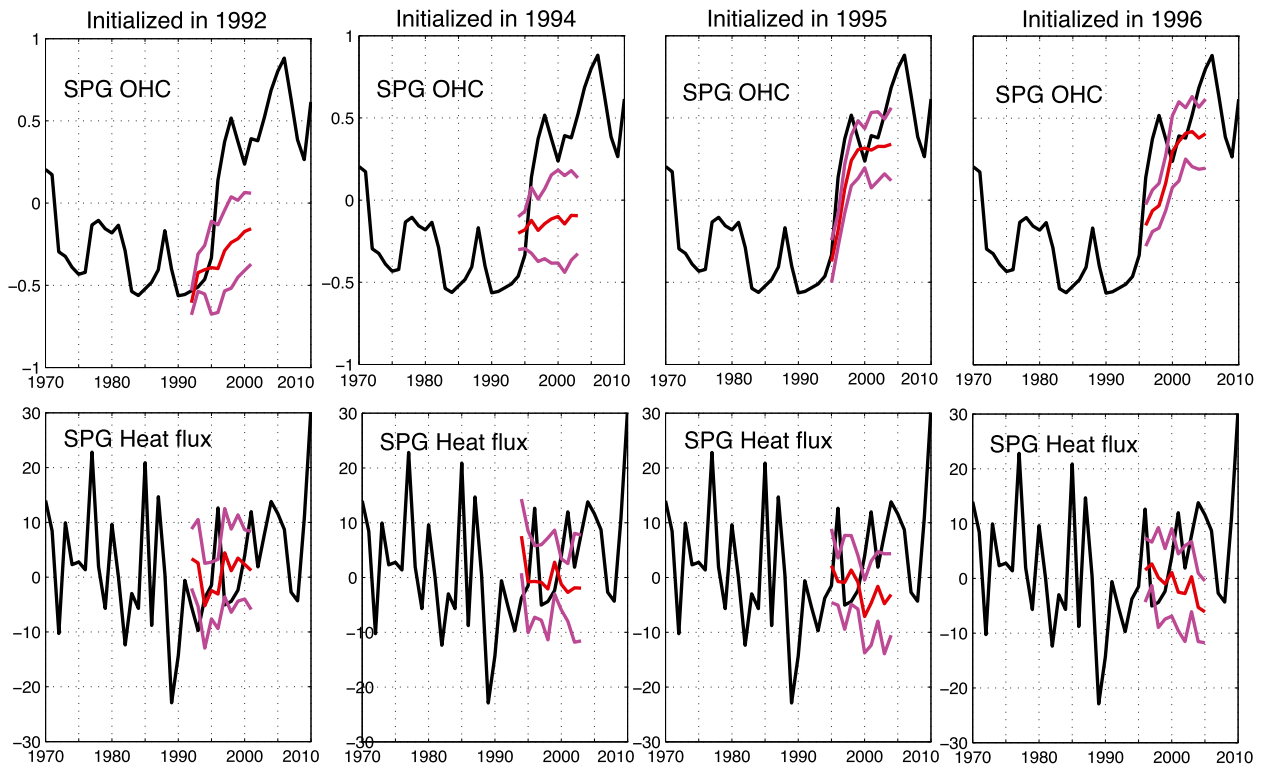


FIG. 7. Ensemble-mean trajectories (red) and their spread (magenta) of North Atlantic SPG OHC anomalies ($^{\circ}\text{C}$) and surface heat flux anomalies counted positive from the atmosphere to the ocean (W m^{-2}) for the predictions initialized between 1992 and 1996. Positive heat flux anomalies correspond to a downward flux (i.e., a warming of the ocean by the atmosphere).

1960 and the mid-1990s followed by an increased salinity (Curry and Mauritzen 2005; Boyer et al. 2005; Reverdin 2010). The freshening during the 1990s has been attributed to NAO-related freshwater fluxes in observations (Visbeck 2003; Reverdin 2010). The salinity variations in ECDA are broadly consistent with observations (Chang et al. 2013), suggesting that initial salinity conditions used in the predictions are at least somewhat realistic, given the paucity of salinity observations available.

The curves of the predicted SPG upper-ocean salinity anomalies (SALT) follow a trajectory very similar to OHC anomalies, with a modest increase for all start dates between 1991 and 1994 and a large increase following the 1995 and 1996 initialization. This suggests that the mechanism in the predictions is such as it involves in-phase changes in temperature and salinity in the SPG following the abrupt warming. The relationship between temperature and salinity is different before the shift, as cold and relatively salty anomalies are predicted by the 1995 hindcast for the first year (Figs. 6 and 8), except in the Labrador Sea where the anomalies are cold and fresh, consistent with observations (Yashayaev 2007). The SPG ensemble-mean SALT anomalies predicted by the 1995 and 1996 hindcasts do not follow the same trajectory as ECDA (Fig. 6), suggesting that other processes that are

not predicted, and possibly not predictable, damp the salinity anomalies in observations. The 1995 ensemble-mean hindcasts are also able to capture the observed weakening of the SPG strength with a remarkable agreement compared to observations (Fig. 6). The predictions at other start dates show a more modest or slower decrease of the SPG strength, consistent with the predicted temperature anomalies. Note that a weakening of the SPG is also found in the uninitialized predictions despite the projected cooling, suggesting a different mechanism than in the initialized hindcasts. This could be partly due to the influence of the positive freshwater anomalies in the forced simulations as precipitation increases in response to larger CO_2 concentrations.

To determine the reason why the 1995 and 1996 predictions are more successful than those initialized the previous years we look at the local surface heat flux predicted after each start date. Given that the NAO switched sign during the winter of 1995/96 and that a negative NAO is associated with a warmer SPG, we check that the warming in the 1995 and 1996 hindcasts does not result, even partially, from a correct (though by chance) prediction of the atmospheric fluxes. Figure 7 shows the atmospheric heat flux predicted by the ensemble-mean hindcasts initialized between 1992 and

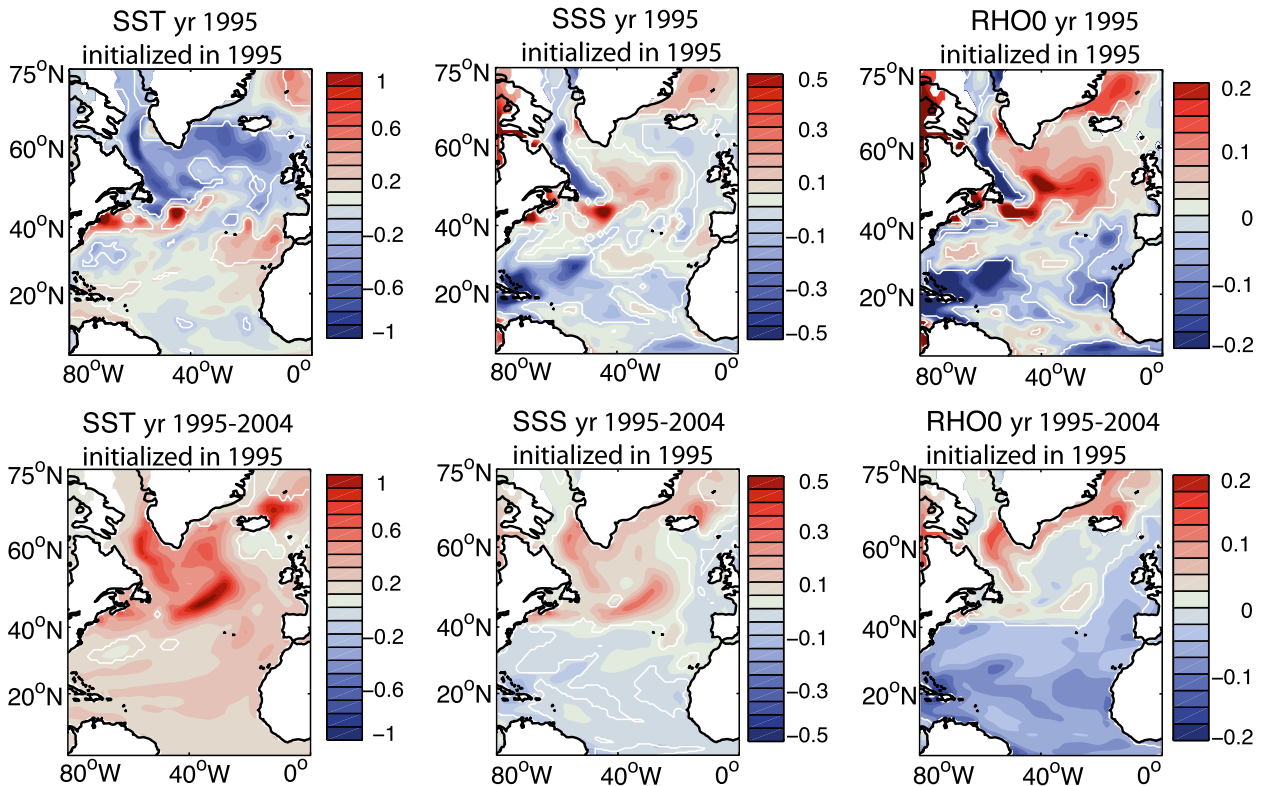


FIG. 8. North Atlantic SST ($^{\circ}\text{C}$), sea surface salinity (SSS) (psu), and surface density (kg m^{-3}) anomalies predicted by the 1995 ensemble-mean hindcast. (top) The first year of the predictions and (bottom) the average over the whole 10-yr hindcast period are shown. White contours indicate statistically significant values at 95%.

1996. None of the forecasts is successful at predicting the positive surface heat flux anomalies in 1996. The 1995 and 1996 ensemble-mean predictions show negative heat fluxes for almost the whole hindcast period, even though the initialized values are positive in 1996. The spatial pattern of heat flux anomalies is similar to the OHC anomalies with the opposite sign (not shown), indicating that the fluxes are damping the warmer temperatures, rather than creating them. Looking at the predictions of sea level pressure (SLP) further shows no skill at predicting the sign of the NAO, as expected. Out of the 10 members of the 1995 hindcasts, 2 predicted a positive (and rather weak) NAO, whereas the other 8 members predicted a neutral or weakly negative NAO (not shown). The successful SPG warming predicted by the 1995 and 1996 forecasts is thus not due to some members skillfully predicting the sign of the NAO.

Comparing the initial conditions in 1995 to those of the previous years indicates larger salinity anomalies along the NAC path in 1995 compared to 1994 and previous years and positive salinity anomalies that are spread to the central and eastern parts of the SPG (not shown). The predictions initialized in early 1995 show positive surface density anomalies for the first year over

most of the SPG, except for the Labrador Sea (Fig. 8). The SPG gets uniformly warm and salty over the 10-yr hindcast period following 1995, a feature not found for prior start dates. Looking at the spatial evolution of temperature anomalies after the 1995 initialization suggests that the warming comes from an increased northward advection of positive anomalies from the subtropics (Fig. 9). The largest increase in OHC and SALT is found first in the eastern SPG, where the influence of the NAC and the wind stress curl are strongest (Reverdin 2010).

The increase of upper-ocean salinity in the 1995 ensemble-mean hindcasts is consistent with salinity anomalies being advected from the subtropics (Fig. 6). None of the other forecasts initialized between 1991 and 1994 shows comparable propagation of OHC and SALT; although an initial strengthening of the NAC is suggested in the predicted first year, the anomalies quickly fade away before reaching the SPG. An enhanced NAC is also found following the 1996 initialization, but the SPG density anomalies are smaller than in 1995 because of the warmer SST anomalies in 1996, as the hindcasts are started just when the NAO switched to a negative phase. The propagation of anomalies from the Subtropical Gyre has been clearly identified in hydrographic

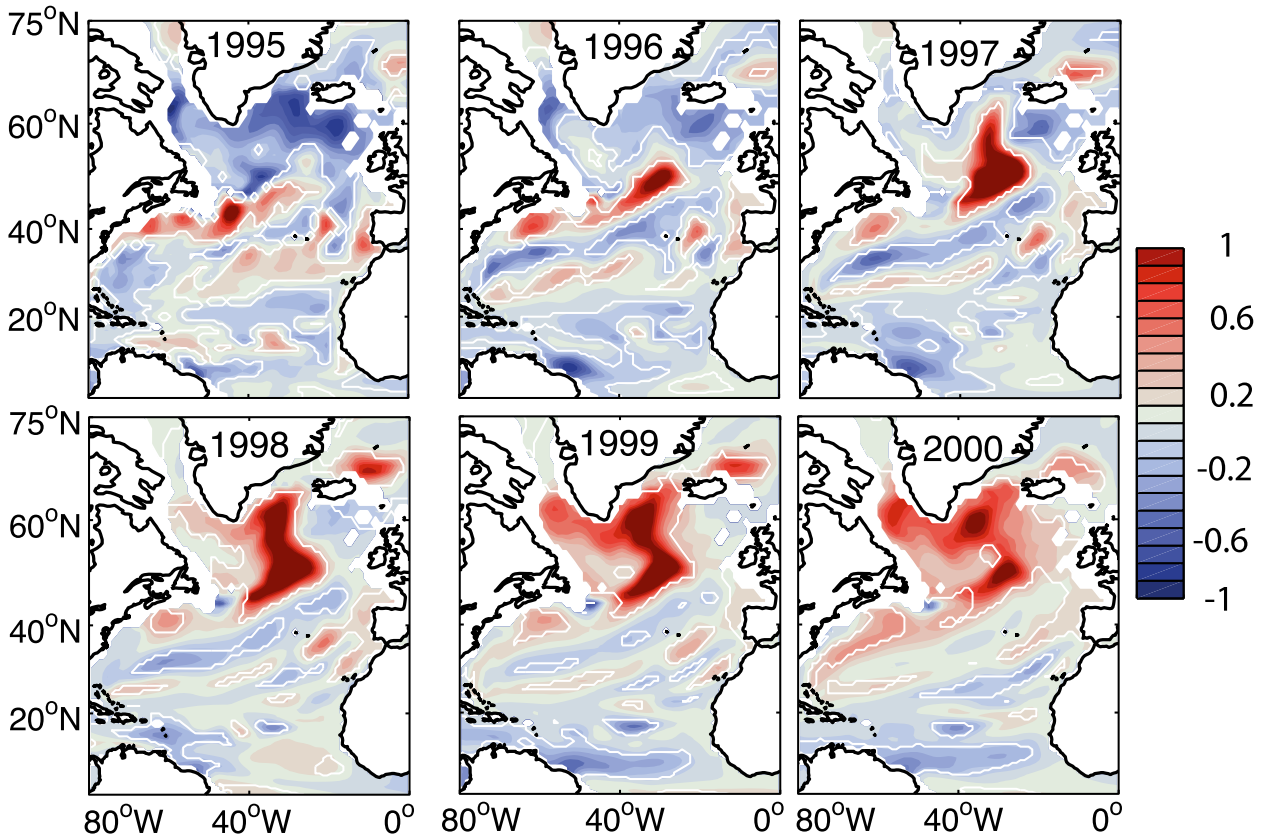


FIG. 9. Evolution of North Atlantic OHC anomalies ($^{\circ}\text{C}$) following the 1995 initialization. White contours indicate statistically significant values at 95%.

data (Bersch 2007; Holliday et al. 2008). Reverdin (2010) stressed that the NAC transport varies as the integral of the NAO forcing in observations (Curry and McCartney 2001), yielding the strongest transport in 1995. Following this mechanism, the 1995 warming and the enhanced SPG salinity would be linked to changes in the barotropic circulation (Hátún et al. 2005). Model studies have also suggested that the decadal warming of the SPG could be due to the lagged response of the AMOC to interdecadal variability of the NAO (Eden and Jung 2001). Both mechanisms could be linked, as is further explored below.

4. Mechanism explaining the success of the retrospective predictions

a. Role of the initial AMOC anomalies

The evolution of OHC anomalies in Fig. 9 suggests an increased northward transport of warm and salty subtropical waters by an enhanced North Atlantic Current following the 1995 initialization. The barotropic streamfunction anomalies predicted over the few years following

the 1995 initialization indicate a weakening of the Subtropical Gyre, a strengthening of the Western Subpolar Gyre, and an enhanced NAC at the boundary between the two gyres with a northeastward extension (Fig. 10a). These anomalies act to weaken and contract the SPG northwestward, favoring a northward advance of warm saline subtropical waters (Fig. 10a). This suggests that the predicted mid-1990s warming was linked to changes in the barotropic circulation.

The NAC is the upper branch of the AMOC, and an increased overturning circulation is usually accompanied by an enhanced transport by the NAC. The predicted changes in the barotropic circulation described in Fig. 10a are associated with an anomalously strong AMOC (Fig. 10b), colder deep temperatures over the depth range of the lower North Atlantic Deep Water (NADW) (Fig. 10c), and a deeper mix in the Labrador region (Figs. 10d, 11). These are all consistent with an enhanced deep-water formation in the Labrador Sea, leading to an intensified North Atlantic Deep Water cell and a subsequently larger southward return flow at depth following the 1995 initialization, which is consistent with the oceanic response to a persistent positive NAO.

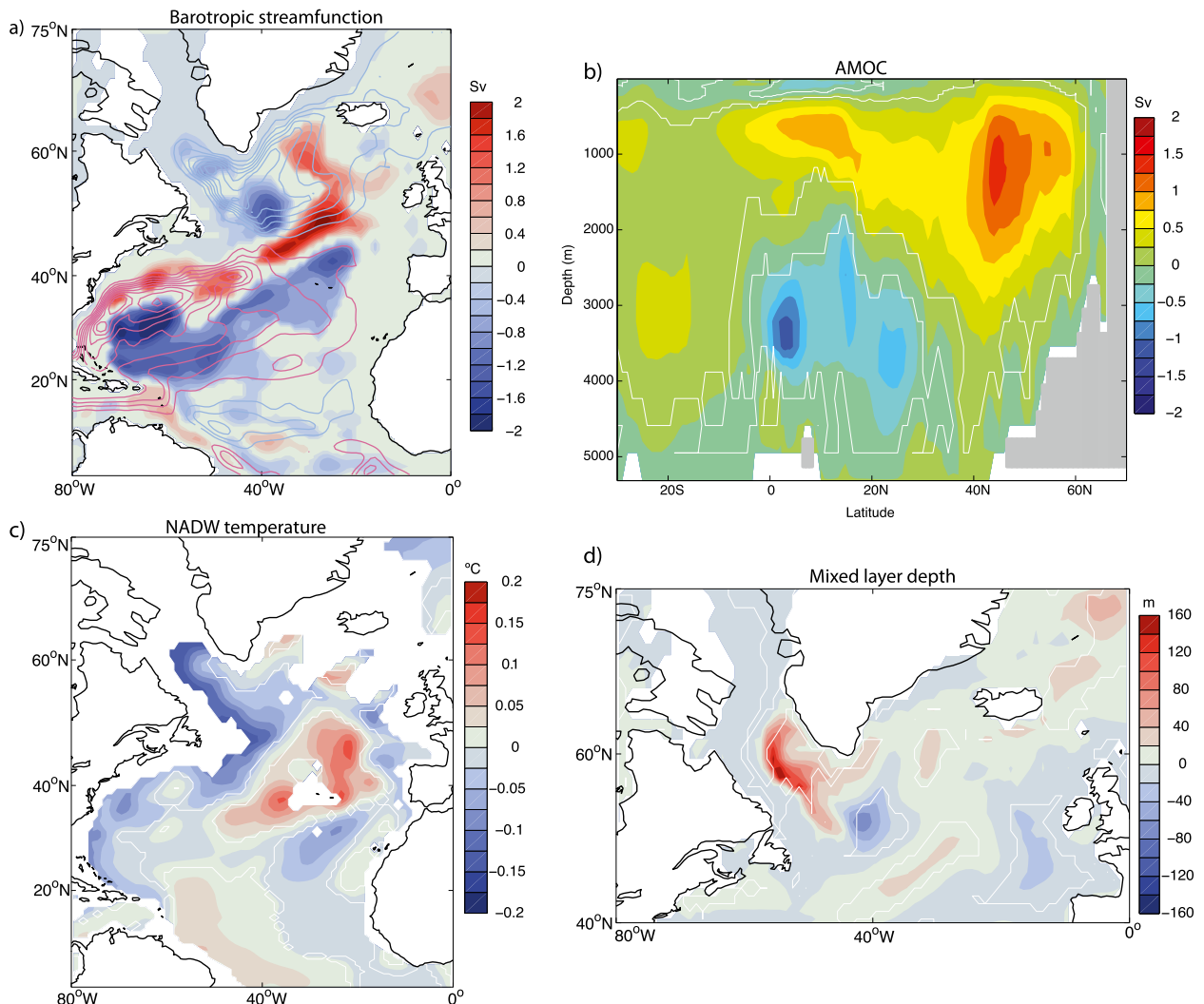


FIG. 10. (a) Barotropic streamfunction anomalies (shaded values) averaged over years 1995–2000 following the 1995 initialization. The mean gyre circulation defined by the 1961–2010 climatology in ECDA is superimposed in red and blue contours for positive and negative values, respectively. Contour interval is every 5 Sv (the zero contour is omitted). (b)–(d) Shading indicates the anomalies averaged over the same period as in (a) for AMOC, with lower NADW temperature defined as the average between 1000 and 2500 m, and mixed layer depth, respectively. In (b)–(d), white contours indicate statistically significant anomalies at 95%. For clarity, only statistically significant anomalies are shaded in (a).

The surface density anomalies predicted by the 1995 hindcasts show negative density anomalies in the Labrador Sea when the ocean is cold and fresh and positive anomalies over the whole Subpolar Gyre for the following years, as warm and salty anomalies spread northward (Figs. 8 and 9). This indicates a strong impact of salinity on density anomalies and hence on deep-water formation in the 1995 hindcasts. Following the 1995 initialization, the mixed layer depth initially increases in the central Subpolar Gyre, which corresponds to the region where the ocean is anomalously cold and salty until 1997 (Fig. 11). The mixed layer depth then decreases in this area and becomes enhanced in the

Labrador Sea from 1998 onward, as warm and salty anomalies have reached the western SPG. The stronger AMOC initialized in 1995 is therefore maintained and further enhanced over the 10-yr hindcast period, as salinity-driven density anomalies maintain deep convection in the SPG. Note that, unlike in the predictions shown in Fig. 11, deep convection in the Labrador Sea stops after 1995 in ECDA, consistent with observations by Lazier et al. (2002). This is because the SPG warming in the ensemble-mean initialized predictions occurs at a slightly slower rate than observed over the first few years following initialization (Fig. 6). Hence, the mechanism in the predictions is delayed by a few years,

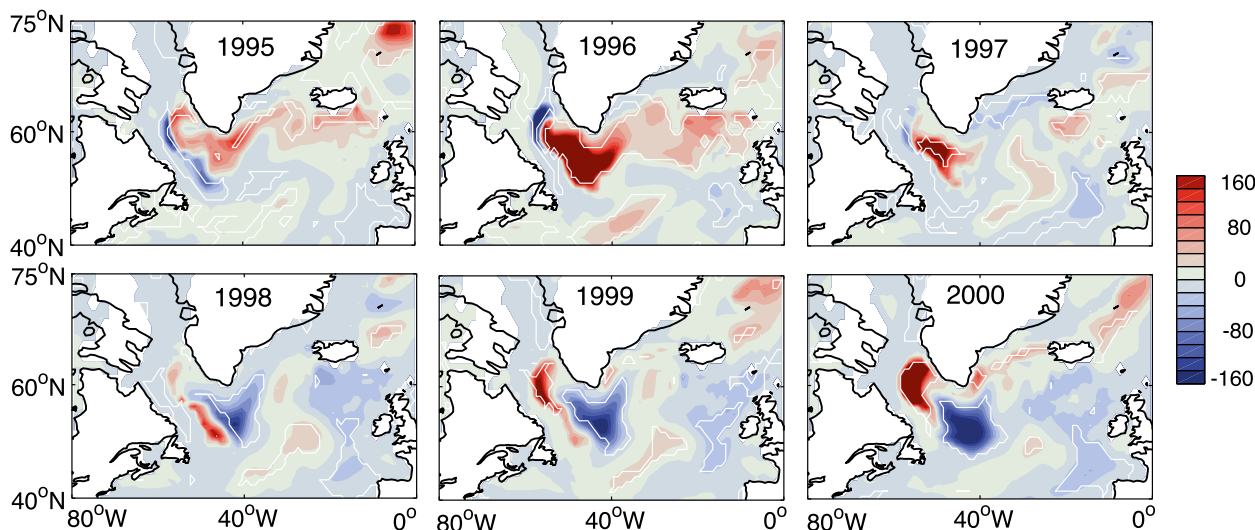


FIG. 11. Evolution of North Atlantic mixed layer depth anomalies (m) following the 1995 initialization. White contours indicate statistically significant values at 95%.

compared to what likely occurred in the real climate system.

The evolution of AMOC anomalies with latitude and time indicates maximum values between 40° and 60°N, peaking in the first three years following initialization and slowly decaying thereafter as they propagate southward (Fig. 12). This southward propagation of AMOC anomalies from the SPG to the Subtropical Gyre can be slowed by the existence of interior pathways (Zhang 2010) and can thus be slightly different in models with increased horizontal resolution (Böning et al. 2006). Broadly, the same time and latitude evolution is found for Atlantic MHT anomalies, with maximum values of about 0.1PW at about 45°N in 1996 at the time the AMOC peaks and a small phase lag north of 50°N. Decomposing the total MHT into its overturning and gyre components confirms the large role of the overturning, in particular south of 50°N (Fig. 12b). It also shows a positive contribution from the horizontal circulation north of 50°N after a couple of years, which explains the phase lag between AMOC and total MHT in the SPG (Fig. 12b). Following Robson et al. (2012b) analysis, we decompose the predicted MHT anomalies into a \overline{VT}' component and a $V'\overline{T}$ component, which represent the advection of temperature anomalies by the mean currents and the anomalous advection of mean temperatures, respectively (Figs. 12d,e). The contribution of $V'\overline{T}$ is initially positive north of 50°N but weak and is only significant between 10° and 20°N. It then increases after 1996 with a pattern very similar to the overturning and total MHT south of 45°N. In contrast, \overline{VT}' is initially positive between 35° and 50°N, which corresponds to the warm anomalies along the NAC path

in Fig. 1a, and then it dominates the MHT in the SPG north of 45°N. This indicates that both \overline{VT}' and $V'\overline{T}$ contribute to the North Atlantic warming, with $V'\overline{T}$ having the largest contribution in the Subtropical Gyre and \overline{VT}' being dominant in the SPG. This is consistent with a warming initiated in the subtropics and advected northward through an enhanced AMOC. None of the hindcasts initialized before 1995 shows positive MHT and AMOC anomalies for the whole hindcast period, as in Fig. 12. The MHT evolution in the 1996 hindcast is comparable to that following the 1995 initialization, except that the AMOC and MHT anomalies have a smaller magnitude and persist for fewer years, as compared to the 1995 hindcast.

We hypothesize that the strong sensitivity to initial conditions can be partly explained by the adjustment time to NAO forcing as described in the following section, as well as to initial conditions used in the predictions, and more specifically, the evolution of SPG salinity in ECDA between 1991 and 1995. The hindcasts initialized in the 1990s prior to 1995 have initial SPG salinity anomalies (both at the surface and integrated over the upper ocean) fresher than climatology. The evolution after initialization indicates an increase in salinity consistent with the increased transport from the subtropics, but in these predictions, the anomalies remain negative (Fig. 6). In contrast, in the 1995 hindcasts, the ocean is initialized with slightly positive salinity anomalies both at the surface and over the upper 600 m, which further increase during the hindcast period (Fig. 8). We hypothesize that these salinity anomalies, which drive denser anomalies over the SPG, maintain a deep mixed layer in the 1995 hindcasts and hence a strong

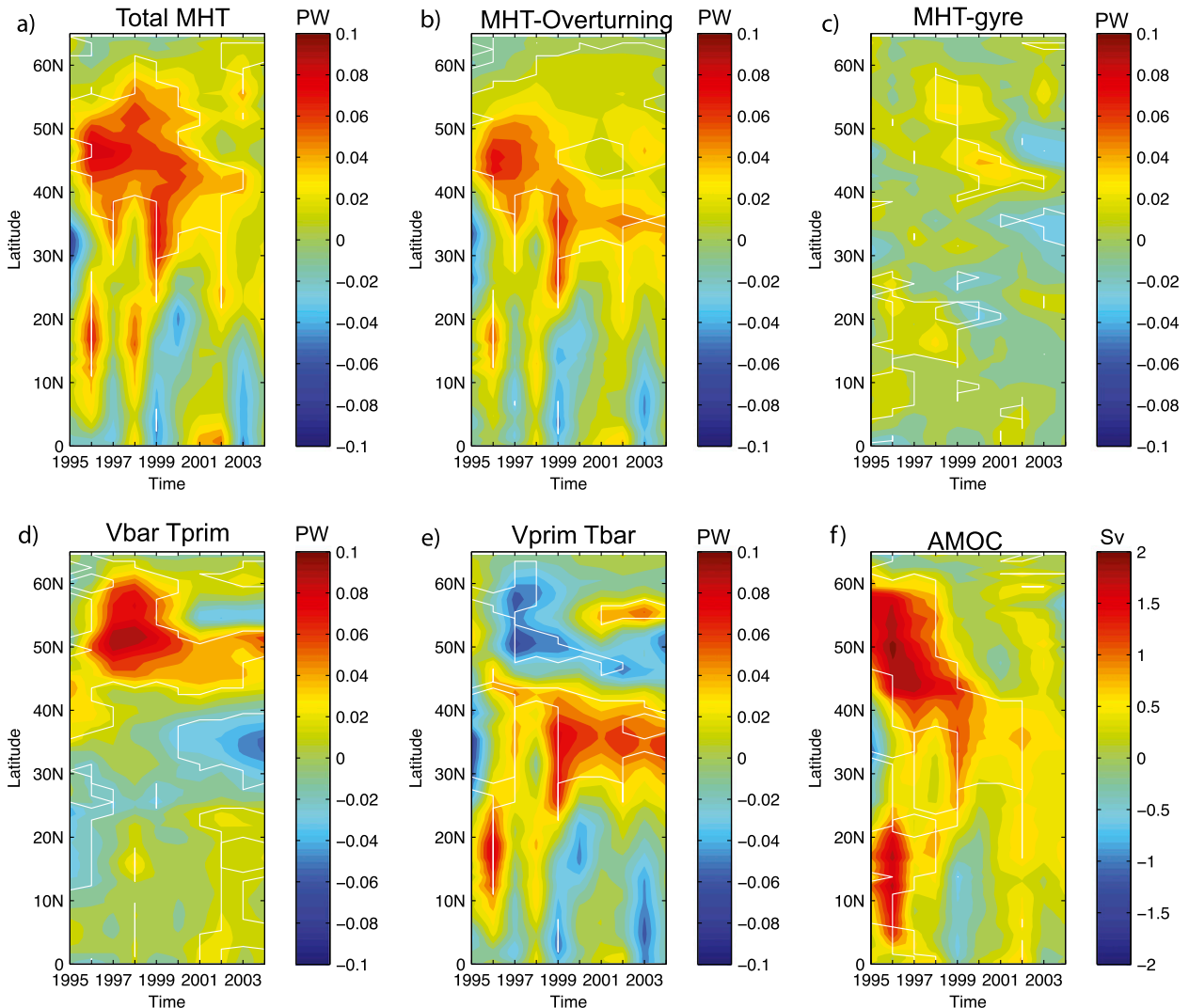


FIG. 12. Time and latitude evolution of (a) MHT anomalies following the 1995 initialization, (b) its overturning, and (c) gyre contributions, and its decomposition into (d) $\bar{V}T'$ and (e) $V'T'$; \bar{V} and \bar{T} correspond to the 1986–2005 climatology of velocity and temperature, respectively, and the prime refers to the anomaly relative to this climatology. The $V'T'$ term is small and not shown. The (f) corresponding AMOC anomalies, defined as the maximum below 500 m, are shown. White contours indicate statistically significant values at 95%.

AMOC and associated heat transport, whereas in the other hindcasts, the anomalies quickly fade away. Whether the variability of salinity anomalies in ECDA between 1991 and 1995 does match actual observations is difficult to assess given the sparse observations. Observations suggest that temperature is the main driver of density changes in the SPG on interannual time scales (Reverdin 2010). Deshayes et al. (2014) showed that the relationship between AMOC and salinity in climate models actually depends on the time scale of interest and on the model's internal variability, stressing the need for additional continuous observations of SPG salinity to fully address this issue. Importantly, for the mechanism described in this study, an increase in the SPG

salinity tends to precede the intensification of the AMOC in CM2.1, as described by Deshayes et al. (2014) for the GFDL CM3 model, where the ocean component is quite similar to that of CM2.1, with the same sensitivity to salinity (not shown).

b. SPG response to persistent positive NAO forcing in CM2.1

The proposed mechanism for the SPG warming, which involves a buildup of positive density anomalies in the SPG in the early 1990s in response to the persistent positive NAO forcing, was based on previous modeling studies of the oceanic adjustment to the observed NAO (Visbeck et al. 2003; Lozier et al. 2008; Lohmann et al. 2009a).

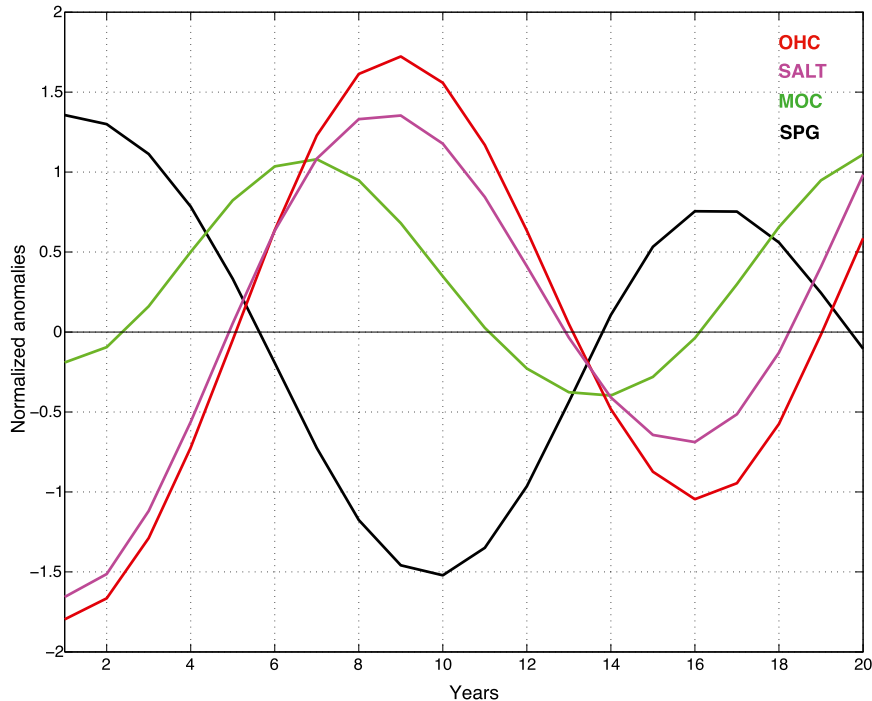


FIG. 13. Time evolution in response to a persistent positive NAO in CM2.1 of the SPG strength index (defined as in Fig. 1), the AMOC maximum at 42°N, and the SPG upper OHC and SALT anomalies. All the time series have been low-pass filtered at 10 yr and normalized.

To better determine the adjustment time scale of the SPG in the CM2.1 initialized predictions, we make use of additional sensitivity experiments in which the models' fluxes at the air–sea interface have been modified. Specifically, extra fluxes of heat, water, and momentum that have the spatial pattern of the regression coefficients associated with a positive phase of the models NAO are added to the ocean. This anomalous NAO-related forcing is applied for 20 years, only in the months of November–March, with a 10-day ramp-up and ramp-down of the forcings at the beginning and end of the period. The application of these extra flux terms is meant to mimic the impact of a persistent positive NAO on the ocean through the surface flux terms. An ensemble of five experiments was conducted, which differ only in their initial conditions taken from periods 50 years apart in the CM2.1 control integration. As we are interested in comparing with the mid-1990s adjustment, we show the results of an experiment that corresponds to an initially cold and strong SPG, as in Fig. 1. The response is then obtained by subtracting a “neutral” experiment defined by the average of five control experiments.

Under persistent positive NAO forcing, the initially strong SPG is, after about 10 years, replaced by a weakening of the SPG (Fig. 13). This change in the gyre strength is caused by the delayed AMOC response to the

formation of intermediate and deep waters in the SPG region. The adjustment results from the thickening of the intermediate layers when the SPG is anomalously cold, leading to an enhanced AMOC and a larger poleward advection of warm water, which in turn induces a thinning of the intermediate layers, reversing the initial state. The spin-up of the AMOC is associated with the poleward advection of warm surface water from the Subtropical Gyre counteracting the local buoyancy forcing in the SPG region. The SPG strength can take up to 10 years to respond to positive NAO conditions. The time scale of this initial adjustment depends on the initial oceanic state. The four other NAO experiments that were done starting from different oceanic states, each 50 years apart, reveal that the increase of the SPG strength in response to a persistent positive NAO is reduced when starting from stronger AMOC initial conditions (not shown), consistent with the results of Lohmann et al. (2009a). The adjustment of temperature and salinity anomalies to a persistent positive NAO and the subsequent changes in the SPG strength are in agreement with the mechanism described by Lohmann et al. (2009b) and are similar to the changes predicted by the 1995 and 1996 hindcasts. The evolution with time of the OHC anomalous pattern is also very similar to the anomalies shown in Fig. 9, which strengthen the validity of the mechanism assessed from the initialized predictions.

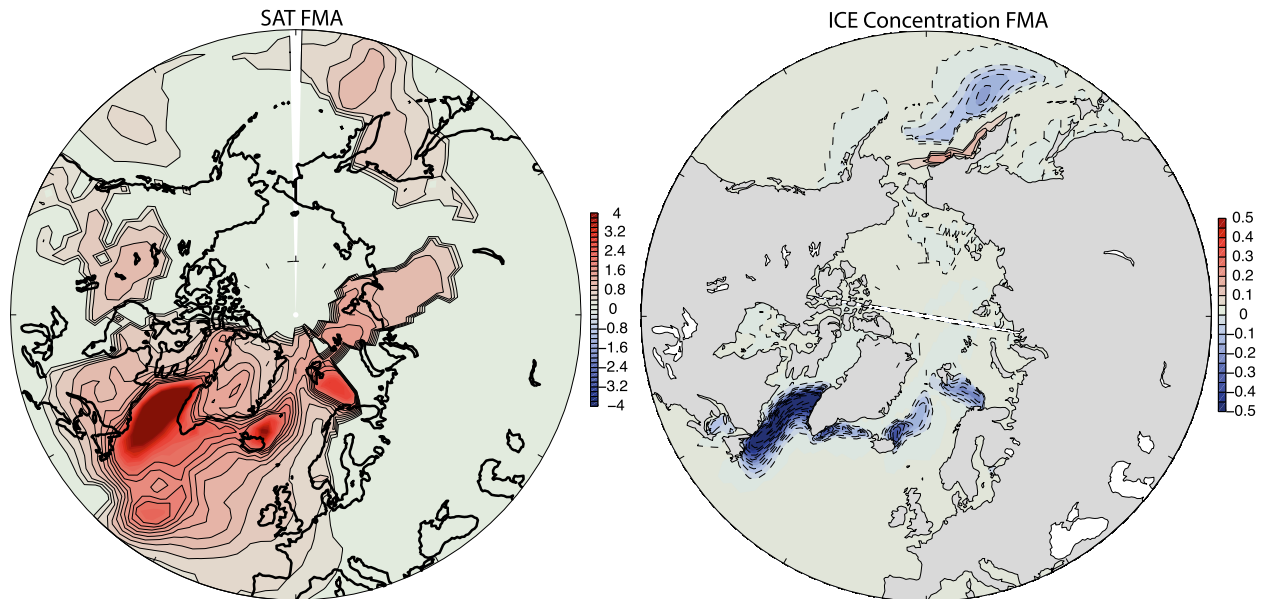


FIG. 14. Winter (FMA) surface air temperature anomalies ($^{\circ}\text{C}$) and sea ice concentration (between 0 and 1) associated with the predicted SPG warming. A detailed description of the method used to define the anomalies is given in the main text. Only the anomalies that are statistically significant at 90% are shown.

5. Predicted climate impacts associated with the SPG warming

In addition to understanding how the SPG upper-ocean temperatures rise in the initialized hindcasts, it is important to identify whether they potentially have any significant climatic impact, in particular over the surrounding land regions. Following the method used by Robson et al. (2012b, 2013), we explore the predictability of the climate anomalies associated with the SPG warming in the GFDL CM2.1 initialized hindcasts by computing the difference between the initialized hindcasts that predict the abrupt warming (the 1995 and 1996 start dates) and those initialized before the warming (between 1960 and 1990). As in Robson et al. (2013), we subtract the same difference from the uninitialized projections to determine the impact of initialization, and we focus on lead 6–10 yr when the impact of initialization is substantially larger than persistence (Fig. 3). The statistical significance of the difference is assessed by using a two-sided t test in which the number of degrees of freedom is defined by the total number of years 6–10, reduced to account for the serial correlation of the time series (Bretherton et al. 1999). Figure 14 shows the winter [February–April (FMA)] surface air temperature (SAT) and sea ice concentration anomalies over the Arctic region. The warming of the SPG extends across the whole pan-Arctic region, with the largest anomalies over the Labrador Sea, the Nordic seas, and the Barents Sea. While only the FMA anomalies are shown, a significant

reduction of sea ice concentration is predicted for all seasons, with the largest anomalies occurring during winter. The Arctic anomalies predicted by the initialized hindcasts that warm abruptly are very similar to those described by Mahajan et al. (2011), which were associated with the natural variations of the AMOC and the AMV in the 1000-yr control simulation of the GFDL CM2.1. Mahajan et al. (2011) suggested that a strengthening of the AMOC, in addition to external forcing, might have contributed to the observed decline of winter sea ice in the Labrador and Nordic seas over the past decades. Our results are consistent with their finding and further suggest that the observed warming of the SPG in the mid-1990s might have contributed to the decline of Arctic sea ice over the following decade.

Besides sea ice, significant seasonal impacts in atmospheric temperature, precipitation, and sea level pressure are predicted by the hindcasts that warm abruptly (Fig. 15). The climate anomalies described in this study can be seen as representative of what could be predicted when a strong warming of the SPG occurs and is predicted. Unlike in Robson et al. (2013), we do not attempt to identify whether these anomalies compare well with observations over the same period. Instead, we discuss the extent to which these climate anomalies are similar to those associated with the AMV published in previous papers. All seasons show warm temperatures over the North Atlantic, associated with enhanced rainfall and low sea level pressure. The warming extends over land to western Europe and North Africa for all seasons.

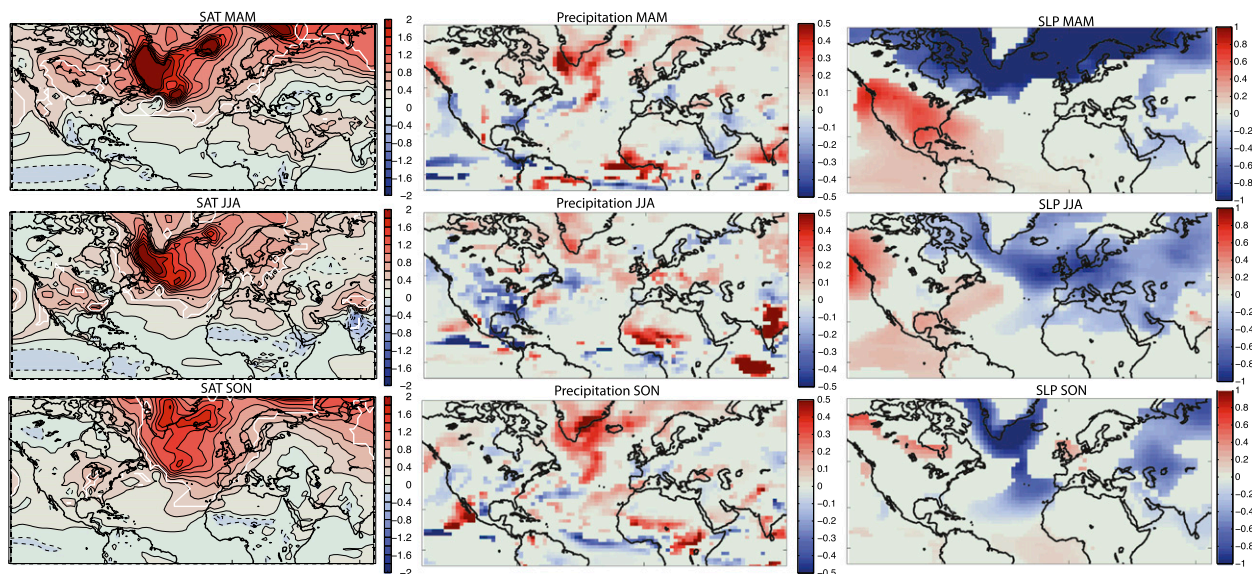


FIG. 15. Seasonal surface air temperature ($^{\circ}\text{C}$), precipitation (mm day^{-1}), and sea level pressure (mb) for anomalies in (top) March–May (MAM), (middle) July–August (JJA), and (bottom) September–November (SON) associated with the predicted SPG abrupt warming. See text for more details on how the anomalies are defined. Only anomalies that are statistically significant at 90% are shown for precipitation and SLP. Significance is indicated by white contours for SAT.

Higher temperatures are found over North America during winter and spring, with anomalies localized over the central and eastern United States during summer and fall, which is consistent with AMV-induced climate anomalies described in Sutton and Hodson (2005). The climate anomalies in Fig. 15 are also consistent with Enfield et al. (2001) and McCabe et al. (2004), who found reduced summer rainfall and increased drought frequency over much of the United States associated with warm conditions in the North Atlantic. In our experiments, the largest precipitation anomalies are found in the tropics, particularly during spring, summer, and fall, with a pattern that indicates a northward shift of the ITCZ. A consistent interhemispheric contrast is found in air temperature; however, the Southern Hemisphere anomalies are weak and not significant (Fig. 15). The SPG mid-1990s warming was suggested to be the driver of increased hurricane frequency in the tropical North Atlantic (Smith et al. 2010; Dunstone et al. 2011), but no evidence of this link is found in our retrospective predictions. Enhanced rainfall is predicted over the Sahel and over India during summer, with the largest precipitation anomalies over these two land regions. Consistent temperature anomalies are predicted over Africa and over the Indian area, with a cooling over south central India and a warming north of it, a dipole characteristic of an increased summer monsoon. These anomalies are consistent with the suggested link between the AMV and the Indian and Sahel rainfall anomalies described in Zhang and Delworth (2006) and Knight et al. (2006).

6. Discussion and conclusions

We analyzed the GFDL CM2.1 decadal predictions that were performed as part of the CMIP5 experiments, focusing on the mid-1990s abrupt warming that occurred in the North Atlantic SPG. This event was unique because it occurred in phase with a reversal of the NAO and was preceded by several years of positive NAO. Because the North Atlantic SPG is a region where the influence of internal variability is larger than external forcing, this event was a good case study to evaluate a prediction system and determine the importance of ocean preconditioning on the ability to predict such an abrupt shift, were it to happen again in the future. We showed that initializing the GFDL CM2.1 coupled system from an estimate of the observed ocean and atmosphere state leads to a large improvement in predicting retrospective changes in SPG upper-ocean temperatures, including the abrupt mid-1990s shift, compared with uninitialized predictions.

Looking at individual start dates prior to the shift, we emphasized that, despite the lack of skill in predicting the phase reversal of the NAO, the ensemble-mean predictions initialized in 1995 and 1996 are able to reproduce the abrupt warming as well as the associated weakening and contraction of the SPG. We analyzed the mechanism responsible for the warming in the successful 1995 and 1996 predictions and showed that both the AMOC and changes in the barotropic circulation play a key role. Unlike the hindcasts initialized between 1991

and 1994, the 1995 and 1996 ensemble-mean hindcasts are started with an intensified AMOC that remains high after initialization for several years. The stronger AMOC is associated with a stronger North Atlantic Current, which increases the transport of warm saline subtropical waters northward toward the Eastern Subpolar Gyre. This leads to a northwestward shift of the Subpolar Front and a spindown and contraction of the SPG that is consistent with observations (Bersch 2002; Häkkinen and Rhines 2004; Hátún et al. 2005; Sarafanov et al. 2008; Holliday et al. 2008). Hence, the warming of the SPG was found to be linked to changes in both the barotropic circulation and the baroclinic overturning circulation. The successful predictions were initialized with a strong AMOC, which persisted as strong because of salinity-driven density anomalies that were associated with a deeper mixed layer in the SPG. We showed that the stronger AMOC drove a larger transport of heat northward toward the SPG, as well as a contribution of the horizontal circulation at higher latitudes. We further showed that the spatial evolution of the ocean temperature anomalies in CM2.1 was consistent with the model's response to a persistent positive NAO. In 1996, the ocean was still preconditioned by the preceding years of positive NAO, but as the NAO reversed to a negative phase during the 1995/96 winter, the predictions initialized in January 1996 had an initially warmer SPG than in January 1995 and a less intense North Atlantic Current consistent with an initially weaker AMOC. That explains the slower predicted warming after the 1996 initialization. In contrast, the hindcasts initialized between 1991 and 1994 do predict an initially stronger NAC, but it does not persist beyond the first year and is not associated with an intensified AMOC and overturning heat transport. Therefore, the predicted warming is not as abrupt as in the 1995 hindcasts and in observations.

Our results are broadly consistent with earlier studies based on independent models and forecast systems (Yeager et al. 2012; Robson et al. 2012b), suggesting some robustness in the proposed mechanism. However, some differences can be stressed, in particular with regard to the role of the barotropic circulation and the timing of the successful predictions. In our forecasts, initialized every year in January, the shift of the SPG could only be predicted when initialized at the beginning of the year it occurred (1995) and the following year (1996), whereas Yeager et al. (2012) argued that a comparable warming would have been retrospectively predicted by every hindcast started between 1991 and 1995. This hypothesis was not verified though, as the CCSM4 hindcasts were initialized only once every 5 years, giving only one start date in the 1990s prior to the shift: namely, 1991. In Robson et al. (2012b), DePreSys was initialized

every year and all the hindcasts started in 1994–96 showed additional skill from initialization because of an intensified AMOC. We investigated the reason for the strong sensitivity to initial oceanic conditions and showed that the initial salinity anomalies in the CM2.1 initialized predictions reflected a saltier SPG in early 1995 than prior to 1995. We argued that these salinity anomalies favored a stronger initial AMOC in 1995 through increased upper-ocean density in the Labrador region. This is supported by the enhanced deep convection and southward transport of cold water along the deep western boundary current that is found after the 1995 and 1996 initializations. Whether the SPG salinity initialized from ECDA corresponds to a realistic state precisely in 1995 is uncertain. Comparison with observational studies by Reverdin (2010) suggests reasonable agreement in the eastern part of the SPG, but salinity observations are too sparse to provide an accurate assessment of the variability of the whole SPG basin. Our coupled assimilation ECDA includes salinity anomalies even when direct observations were not available, through the T - S relationship and altimetry information (Chang et al. 2011a,b), but an accurate validation requires more direct observations. In observations, interannual variations in SPG density are mainly temperature driven (Reverdin 2010), unlike what is found in our predictions. This is a key issue, as a number of climate models show a different sensitivity of the Atlantic circulation to salinity (Frankignoul et al. 2009; Hazeleger et al. 2013; Deshayes et al. 2014). The role of salinity was not specifically addressed in previous studies that assessed the predictive skill of the mid-1990s SPG warming (Yeager et al. 2012; Robson et al. 2012b). Further, salinity was restored in the NCAR Common Ocean–Ice Reference Experiments (CORE) simulation that provided the initial conditions for the CCSM4 decadal predictions analyzed by Yeager et al. (2012), which likely impacted the role of salinity on the SPG variability in their predictions. The importance of salinity initial conditions stressed by Hazeleger et al. (2013) should be assessed in a larger subset of CMIP5 prediction models to identify whether its importance is a robust feature.

Our results show that the observed changes in the SPG strength and shape could be predicted in the initialized experiments that have a strong initial AMOC and NAC. Our 1995 and 1996 initialized hindcasts show that the advection of warm salty waters by the enhanced NAC transport leads a spindown and contraction of the SPG, which supports the modeling study of Hátún et al. (2005), who related the mid-1990s decline and contraction of the SPG to a larger amount of subtropical water advected northward. They are also consistent with Wouters et al. (2013), who showed that the SPG strength could be predicted up to two years ahead in the EC-Earth

Consortium (EC-EARTH) initialized hindcasts, although this study did not focus on the mid-1990s shift in particular. The weakening and contraction of the SPG were investigated in the decadal prediction analyses of Robson et al. (2012b) and Yeager et al. (2012). Further studies would be useful to determine whether abrupt changes in the barotropic SPG circulation can be predicted by other forecast systems.

We investigated the climate impacts associated with the predictions that successfully captured the mid-1990s warming and found significant anomalies over the Arctic, North American, and European regions. We showed that the oceanic SPG warming extended to the whole pan-Arctic region, leading to a reduction of sea ice concentration over the Labrador Sea, the Nordic seas, and the Barents Sea, with the strongest anomalies occurring during winter. These impacts were similar to those associated with the internal variability of the AMOC in CM2.1 (Mahajan et al. 2011), which suggests that initializing the AMOC could improve predictions of Arctic sea ice extent that are not due to external forcing. The abrupt SPG warming was associated with significant climate anomalies in the tropics, with enhanced precipitation over the tropical North Atlantic that extended to the Sahel region and less precipitation south of the equator, indicating a northward shift of the ITCZ. These climate anomalies explain about 5% to 10% of the seasonal variance. Warmer temperatures and lower sea level pressure anomalies were also predicted over North America, western Europe, and North Africa, as well as an enhanced warming over the central and eastern United States during summer and fall. Although we did not validate these predictions directly against observations, the climate anomalies identified in the North and tropical Atlantic are consistent with observational and modeling studies that isolated the seasonal climate impacts of the observed AMV SST pattern (Delworth and Mann 2000; Enfield et al. 2001; McCabe et al. 2004; Sutton and Hodson 2005; Knight et al. 2005, 2006; Zhang and Delworth 2006; Msadek and Frankignoul 2009). Comparable climate impacts have been found in the Met Office DePreSys system (Robson et al. 2013), but the significant rainfall anomalies predicted over the Sahel by our hindcasts were not found in DePreSys, which can be attributed to atmospheric deficiencies of the Hadley Centre Coupled Model, version 3 (HadCM3) (Knight et al. 2006). To our knowledge, our study is also the first to report Arctic impacts associated with the prediction of the mid-1990s SPG warming.

A larger positive AMOC anomaly was found between 1991 and 1995 in the initial conditions of the NCAR CORE simulation (Yeager et al. 2012) and DePreSys (Robson et al. 2012b) compared with ECDA, which was

used in this study. ECDA shows a less coherent AMOC structure than other systems, which can be attributed to the strong observational constraint that is imposed (Zhang et al. 2007). One can make the choice to constrain an assimilation system less (e.g., by rejecting more data) and get an AMOC that looks more like that simulated by an ocean-forced model, which is not the choice that was made in ECDA. The similarity of our results with those of Yeager et al. (2012) and Robson et al. (2012b) indicates that this does not have a strong impact on the ability to predict the mid-1990s shift. However, details in the predicted mechanism and timing of the response can be influenced by this choice, as it can affect AMOC initialization. Different assimilation methods were used in the models that contributed to the CMIP5 decadal prediction experiments, some based on full assimilation (e.g., CM2.1 and CCSM4 predictions), others on anomaly assimilation (e.g., DePreSys). These differences could impact the evolution of the hindcasts (Robson 2010; Bellucci et al. 2013). ECDA initial conditions were produced by a coupled assimilation method in which both the ocean and the atmosphere were constrained by observations, providing balanced initial conditions. This differs substantially from the CCSM4 forecast system used by Yeager et al. (2012), in which the initial conditions were obtained from a CORE-forced ocean–sea ice model in which the observed atmospheric state was prescribed, the ocean feedbacks limited, and no oceanic observations were directly assimilated. In Robson et al. (2012b), DePreSys was constrained by both atmospheric and oceanic observations but in an uncoupled way (i.e., the assimilation was done separately for the atmospheric and oceanic component). While understanding the source of these differences was outside of the scope of this work, assessing the sensitivity of the predictions to differences in the initialization methods remains to be explored.

Model biases remain a fundamental issue in the analysis of initialized decadal predictions because coupled models tend to drift toward their own mean state, which can be far from observations. In particular, coarse-resolution models tend to have a pathway for the subtropical water moving north that is too northerly, thereby favoring a warming and a subsequent weakening of the SPG. In this study, a lead-dependent climatology was removed from the initialized predictions to remove part of the drift. However, anomalies were defined by making the strong assumption that the lead-dependent climatology was stationary in time. Potential impacts of the nonstationary observing system on the skill assessment have been outlined by Kumar et al. (2012) and Vecchi et al. (2013) and have to be better characterized.

In most CMIP5 models, decadal skill was limited to specific regions like the North Atlantic, which is characterized by marked decadal variability (Goddard et al. 2013). It is worth noting that even a simple persistence forecast model can give high skill in predicting ocean temperature anomalies in this region, given the large inertia of the ocean in the North Atlantic. Our case study analysis highlights that initialized dynamical models can bring additional value by predicting shifts like the mid-1990s warming that a persistence forecast model cannot capture. Predicting specific events like this shift, even if they are very localized, could improve the prediction of larger-scale climate impacts given the teleconnections associated with the North Atlantic variability. Data assimilation is expected to contribute to a reduction of the uncertainty compared to the free-running model (Balmaseda et al. 2007); however, initialization of decadal predictions is an emerging field that can benefit from future progress. While one needs to keep in mind that predictability will be ultimately limited by the chaotic nature of the climate system (Lorenz 1963; Balaji 2013), perfect model studies suggest a potential for skill above that currently found in the initialized CMIP5 experiments (Msadek et al. 2010; Wouters et al. 2013). The encouraging skill identified in this study should therefore not be considered as an upper limit of predictability, as improvement in both coupled models and initialization methods can be expected to lead to better predictions in the future.

Acknowledgments. We thank Tim Merlis and Charles Stock for their comments on an early version of the paper. We are grateful to the three anonymous reviewers for their thoughtful comments, which helped to improve the manuscript. We also thank the editor for his patience while waiting for our revisions.

REFERENCES

- Anderson, J. L., 2001: An ensemble adjustment Kalman filter for data assimilation. *Mon. Wea. Rev.*, **129**, 2884–2903, doi:10.1175/1520-0493(2001)129<2884:AEAKFF>2.0.CO;2.
- Balaji, V., 2013: Scientific computing in the age of complexity. *XRDS*, **19**, 12–17, doi:10.1145/2425676.2425684.
- Balmaseda, M., D. Anderson, and A. Vidard, 2007: Impact of Argo on analyses of the global ocean. *Geophys. Res. Lett.*, **34**, L16605, doi:10.1029/2007GL030452.
- Bellucci, A., and Coauthors, 2013: Decadal climate predictions with a coupled OAGCM initialized with oceanic reanalyses. *Climate Dyn.*, **40**, 1483–1497, doi:10.1007/s00382-012-1468-z.
- Bersch, M., 2002: North Atlantic Oscillation-induced changes of the upper layer circulation in the northern North Atlantic Ocean. *J. Geophys. Res.*, **107**, 3156, doi:10.1029/2001JC000901.
- , 2007: Recent changes of the thermohaline circulation in the subpolar North Atlantic. *Ocean Dyn.*, **57**, 223–235, doi:10.1007/s10236-007-0104-7.
- Boer, G. J., 2004: Long time-scale potential predictability in an ensemble of coupled climate models. *Climate Dyn.*, **23**, 29–44, doi:10.1007/s00382-004-0419-8.
- , 2011: Decadal potential predictability of twenty-first century climate. *Climate Dyn.*, **36**, 1119–1133, doi:10.1007/s00382-010-0747-9.
- Böning, C. W., M. Scheinert, J. Dengg, A. Biastoch, and A. Funk, 2006: Decadal variability of subpolar gyre transport and its reverberation in the North Atlantic overturning. *Geophys. Res. Lett.*, **33**, L21S01, doi:10.1029/2006GL026906.
- Boyer, T. P., S. Levitus, J. I. Antonov, R. A. Locarnini, and H. E. Garcia, 2005: Linear trends in salinity for the World Ocean, 1955–1998. *Geophys. Res. Lett.*, **32**, L01604, doi:10.1029/2004GL021791.
- , and Coauthors, 2009: World Ocean Database 2009. NOAA Atlas NESDIS 66, 217 pp. [Available online at ftp://ftp.nodc.noaa.gov/pub/WOD09/DOC/wod09_intro.pdf.]
- Branstator, G., H. Teng, G. A. Meehl, M. Kimoto, J. R. Knight, M. Latif, and A. Rosati, 2012: Systematic estimates of initial-value decadal predictability for six AOGCMs. *J. Climate*, **25**, 1827–1846, doi:10.1175/JCLI-D-11-00227.1.
- Bretherton, C. S., M. Widmann, V. P. Dymnikov, J. M. Wallace, and I. Bladé, 1999: The effective number of spatial degrees of freedom of a time-varying field. *J. Climate*, **12**, 1990–2009, doi:10.1175/1520-0442(1999)012<1990:TENOSD>2.0.CO;2.
- Cassou, C., L. Terray, J. W. Hurrell, and C. Deser, 2004: North Atlantic winter climate regimes: Spatial asymmetry, stationarity with time, and oceanic forcing. *J. Climate*, **17**, 1055–1068, doi:10.1175/1520-0442(2004)017<1055:NAWCRS>2.0.CO;2.
- Chang, Y.-S., A. Rosati, and S. Zhang, 2011a: A construction of pseudo salinity profiles for the global ocean: Method and evaluation. *J. Geophys. Res.*, **116**, C02002, doi:10.1029/2010JC006386.
- , S. Zhang, and A. Rosati, 2011b: Improvement of salinity representation in an ensemble coupled data assimilation system using pseudo salinity profiles. *Geophys. Res. Lett.*, **38**, L13609, doi:10.1029/2011GL048064.
- , —, —, T. L. Delworth, and W. F. Stern, 2013: An assessment of oceanic variability for 1960–2010 from the GFDL ensemble coupled data assimilation. *Climate Dyn.*, **40**, 775–803, doi:10.1007/s00382-012-1412-2.
- Cheng, W., J. C. H. Chiang, and S. Zhang, 2013: Atlantic meridional overturning circulation (AMOC) in CMIP5 models: RCP and historical simulations. *J. Climate*, **26**, 7187–7197, doi:10.1175/JCLI-D-12-00496.1.
- Curry, R. G., and M. S. McCartney, 2001: Ocean gyre circulation changes associated with the North Atlantic Oscillation. *J. Phys. Oceanogr.*, **31**, 3374–3400, doi:10.1175/1520-0485(2001)031<3374:OGCCAW>2.0.CO;2.
- , and C. Mauritzen, 2005: Dilution of the northern North Atlantic Ocean in recent decades. *Science*, **308**, 1772–1774, doi:10.1126/science.1109477.
- Delworth, T. L., and M. E. Mann, 2000: Observed and simulated multidecadal variability in the Northern Hemisphere. *Climate Dyn.*, **16**, 661–676, doi:10.1007/s003820000075.
- , and Coauthors, 2006: GFDL's CM2 global coupled climate models. Part I: Formulation and simulation characteristics. *J. Climate*, **19**, 643–674, doi:10.1175/JCLI3629.1.
- Deshayes, J., and C. Frankignoul, 2008: Simulated variability of the circulation in the North Atlantic from 1953 to 2003. *J. Climate*, **21**, 4919–4933, doi:10.1175/2008JCLI1882.1.
- , R. Curry, and R. Msadek, 2014: CMIP5 model intercomparison of freshwater budget and circulation in the

- North Atlantic. *J. Climate*, **27**, 3298–3317, doi:10.1175/JCLI-D-12-00700.1.
- Doblas-Reyes, F. J., M. A. Balmaseda, A. Weisheimer, and T. N. Palmer, 2011: Decadal climate prediction with the European Centre for Medium-Range Weather Forecasts coupled forecast system: Impact of ocean observations. *J. Geophys. Res.*, **116**, D19111, doi:10.1029/2010JD015394.
- Dunstone, N. J., D. M. Smith, and R. Eade, 2011: Multi-year predictability of the tropical Atlantic atmosphere driven by the high latitude North Atlantic Ocean. *Geophys. Res. Lett.*, **38**, L14701, doi:10.1029/2011GL047949.
- Eden, C., and T. Jung, 2001: North Atlantic interdecadal variability: Oceanic response to the North Atlantic Oscillation (1865–1997). *J. Climate*, **14**, 676–691, doi:10.1175/1520-0442(2001)014<0676:NAIVOR>2.0.CO;2.
- , and J. Willebrand, 2001: Mechanism of interannual to decadal variability of the North Atlantic Circulation. *J. Climate*, **14**, 2266–2280, doi:10.1175/1520-0442(2001)014<2266:MOITDV>2.0.CO;2.
- Enfield, D. B., A. M. Mestas-Núñez, and P. J. Trimble, 2001: The Atlantic multidecadal oscillation and its relation to rainfall and river flows in the continental U.S. *Geophys. Res. Lett.*, **28**, 2077–2080, doi:10.1029/2000GL012745.
- Escudier, R., J. Mignot, and D. Swingedouw, 2013: A 20-year coupled ocean–sea ice–atmosphere variability mode in the North Atlantic in an AOGCM. *Climate Dyn.*, **40**, 619–636, doi:10.1007/s00382-012-1402-4.
- Flatau, M., L. Talley, and P. P. Niiler, 2003: The North Atlantic Oscillation, surface current velocities, and SST changes in the subpolar North Atlantic. *J. Climate*, **16**, 2355–2369, doi:10.1175/2787.1.
- Frankcombe, L. M., A. von der Heydt, and H. Dijkstra, 2010: North Atlantic multidecadal climate variability: An investigation of dominant time scales and processes. *J. Climate*, **23**, 3626–3638, doi:10.1175/2010JCLI3471.1.
- Frankignoul, C., and K. Hasselmann, 1977: Stochastic climate models, Part II. Application to sea-surface temperature anomalies and thermocline variability. *Tellus*, **29A**, 289–305, doi:10.1111/j.2153-3490.1977.tb00740.x.
- , J. Deshayes, and R. Curry, 2009: The role of salinity in the decadal variability of the North Atlantic meridional overturning circulation. *Climate Dyn.*, **33**, 777–793, doi:10.1007/s00382-008-0523-2.
- García-Serrano, J., F. J. Doblas-Reyes, and C. A. S. Coelho, 2012: Understanding Atlantic multi-decadal variability prediction skill. *Geophys. Res. Lett.*, **39**, L18708, doi:10.1029/2012GL053283.
- Goddard, L., and Coauthors, 2013: A verification framework for interannual-to-decadal predictions experiments. *Climate Dyn.*, **40**, 245–272, doi:10.1007/s00382-012-1481-2.
- Griffies, S. M., and K. Bryan, 1997: A predictability study of simulated North Atlantic multidecadal variability. *Climate Dyn.*, **13**, 459–487, doi:10.1007/s003820050177.
- Guemas, V., S. Corti, J. García-Serrano, F. Doblas-Reyes, M. A. Balmaseda, and L. Magnusson, 2013: The Indian Ocean: The region of highest skill worldwide in decadal climate prediction. *J. Climate*, **26**, 726–739, doi:10.1175/JCLI-D-12-00049.1.
- Häkkinen, S., and P. B. Rhines, 2004: Decline of subpolar North Atlantic circulation during the 1990s. *Science*, **304**, 555–559, doi:10.1126/science.1094917.
- Hanawa, K., P. Raul, R. Bailey, A. Sy, and M. Szabados, 1995: A new depth–time equation for Sippican or TSK T-7, T-6 and T-4 expendable bathythermographs (XBT). *Deep Sea Res. I*, **42**, 1423–1451, doi:10.1016/0967-0637(95)97154-Z.
- Hátún, H., A. B. Sandø, H. Drange, B. Hansen, and H. Valdimarsson, 2005: Influence of the Atlantic subpolar gyre on the thermohaline circulation. *Science*, **309**, 1841–1844, doi:10.1126/science.1114777.
- , and Coauthors, 2009: Large bio-geographical shifts in the north-eastern Atlantic Ocean: From the subpolar gyre, via plankton, to blue whiting and pilot whales. *Prog. Oceanogr.*, **80**, 149–162, doi:10.1016/j.pocean.2009.03.001.
- Hazeleger, W., and Coauthors, 2013: Predicting multiyear North Atlantic Ocean variability. *J. Geophys. Res. Oceans*, **118**, 1087–1098, doi:10.1002/jgrc.20117.
- Holliday, N. P., and Coauthors, 2008: Reversal of the 1960s to 1990s freshening trend in the northeast North Atlantic and Nordic Seas. *Geophys. Res. Lett.*, **35**, L03614, doi:10.1029/2007GL032675.
- Hurrell, J. W., 1995: Decadal trends in the North Atlantic Oscillation: Regional temperatures and precipitation. *Science*, **269**, 676–679, doi:10.1126/science.269.5224.676.
- , Y. Kushnir, G. Ottersen, and M. Visbeck, 2003: An overview of the North Atlantic Oscillation. *The North Atlantic Oscillation: Climatic Significance and Environmental Impact*, *Geophys. Monogr.*, Vol. 134, Amer. Geophys. Union, 1–35.
- ICPO, 2011: Data and bias correction for decadal climate predictions. International CLIVAR Project Office, CLIVAR Publication Series 150, 6 pp. [Available online at http://www.wcrp-climate.org/decadal/references/DCPP_Bias_Correction.pdf.]
- Ingleby, B., and M. Huddleston, 2007: Quality control of ocean temperature and salinity profiles—Historical and real-time data. *J. Mar. Sci.*, **65**, 158–175, doi:10.1016/j.jmarsys.2005.11.019.
- Johns, W. E., and Coauthors, 2011: Continuous, array-based estimates of Atlantic Ocean heat transport at 26.5°N. *J. Climate*, **24**, 2429–2449, doi:10.1175/2010JCLI3997.1.
- Kalnay, E., and Coauthors, 1996: The NCEP/NCAR 40-Year Reanalysis Project. *Bull. Amer. Meteor. Soc.*, **77**, 437–471, doi:10.1175/1520-0477(1996)077<0437:TNYRP>2.0.CO;2.
- Keenlyside, N. S., M. Latif, J. Jungclauss, L. Kornbluh, and E. Roeckner, 2008: Advancing decadal-scale climate prediction in the North Atlantic sector. *Nature*, **453**, 84–88, doi:10.1038/nature06921.
- Keyl, F., and M. Wolff, 2008: Environmental variability and fisheries: What can models do? *Rev. Fish Biol. Fish.*, **18**, 273–299, doi:10.1007/s11160-007-9075-5.
- Kim, H.-K., P. J. Webster, and J. A. Curry, 2012: Evaluation of short-term climate change prediction in multi-model CMIP5 decadal hindcasts. *Geophys. Res. Lett.*, **39**, L10701, doi:10.1029/2012GL051644.
- Kizu, S., H. Yoritaka, and K. Hanawa, 2005: A new fall-rate equation for T-5 expendable bathythermograph (XBT) by TSK. *J. Oceanogr.*, **61**, 115–121, doi:10.1007/s10872-005-0024-4.
- Knight, J. R., R. J. Allan, C. K. Folland, M. Vellinga, and M. E. Mann, 2005: A signature of persistent natural thermohaline circulation cycles in observed climate. *Geophys. Res. Lett.*, **32**, L20708, doi:10.1029/2005GL024233.
- , C. K. Folland, and A. A. Scaife, 2006: Climate impacts of the Atlantic multidecadal oscillation. *Geophys. Res. Lett.*, **33**, L17706, doi:10.1029/2006GL026242.
- Kumar, A., M. Chen, L. Zhang, W. Wang, Y. Xue, C. Wen, L. Marx, and B. Huang, 2012: An analysis of the non-stationarity in the bias of sea surface temperature forecasts for the NCEP Climate Forecast System (CFS) version 2. *Mon. Wea. Rev.*, **140**, 3003–3016, doi:10.1175/MWR-D-11-00335.1.
- Kwon, Y.-O., and C. Frankignoul, 2012: Stochastically-driven multidecadal variability of the Atlantic meridional overturning

- circulation in CCSM3. *Climate Dyn.*, **38**, 859–876, doi:10.1007/s00382-011-1040-2.
- Lazier, J., R. Hendry, A. Clarke, I. Yashayaev, and P. Rhines, 2002: Convection and restratification in the Labrador Sea, 1990–2000. *Deep-Sea Res. I*, **49**, 1819–1835, doi:10.1016/S0967-0637(02)00064-X.
- Levitus, S., J. I. Antonov, and T. P. Boyer, 2005: Warming of the World Ocean, 1955–2003. *Geophys. Res. Lett.*, **32**, L02604, doi:10.1029/2004GL021592.
- , —, —, R. A. Locarnini, H. E. Garcia, and A. V. Mishonov, 2009: Global ocean heat content 1955–2008 in light of recently revealed instrumentation problems. *Geophys. Res. Lett.*, **36**, L07608, doi:10.1029/2008GL037155.
- Lohmann, K., H. Drange, and M. Bentsen, 2009a: A possible mechanism for the strong weakening of the North Atlantic subpolar gyre in the mid-1990s. *Geophys. Res. Lett.*, **36**, L15602, doi:10.1029/2009GL039166.
- , —, and —, 2009b: Response of the North Atlantic subpolar gyre to persistent North Atlantic Oscillation like forcing. *Climate Dyn.*, **32**, 273–285, doi:10.1007/s00382-008-0467-6.
- Lorenz, E. N., 1963: Deterministic nonperiodic flow. *J. Atmos. Sci.*, **20**, 130–141, doi:10.1175/1520-0469(1963)020<0130:DNF>2.0.CO;2.
- Lozier, M. S., S. Leadbetter, R. G. Williams, V. Roussenov, M. S. C. Reed, and N. J. Moore, 2008: The spatial pattern and mechanisms of heat-content change in the North Atlantic. *Science*, **319**, 800–803, doi:10.1126/science.1146436.
- Mahajan, S., R. Zhang, and T. L. Delworth, 2011: Impact of the Atlantic meridional overturning circulation (AMOC) on Arctic surface air temperature and sea ice variability. *J. Climate*, **24**, 6573–6581, doi:10.1175/2011JCLI4002.1.
- McCabe, G. J., M. A. Palecki, and J. L. Betancourt, 2004: Pacific and Atlantic Ocean influences on multidecadal drought frequency in the United States. *Proc. Natl. Acad. Sci. USA*, **101**, 4136–4141, doi:10.1073/pnas.0306738101.
- Meehl, G. A., and Coauthors, 2009: Decadal prediction: Can it be skillful? *Bull. Amer. Meteor. Soc.*, **90**, 1467–1485, doi:10.1175/2009BAMS2778.1.
- , and Coauthors, 2014: Decadal climate prediction: An update from the trenches. *Bull. Amer. Meteor. Soc.*, **95**, 243–267, doi:10.1175/BAMS-D-12-00241.1.
- Mehta, V., and Coauthors, 2011: Decadal climate predictability and prediction: Where are we? *Bull. Amer. Meteor. Soc.*, **92**, 637–640, doi:10.1175/2010BAMS3025.1.
- Meinshausen, M., and Coauthors, 2011: The RCP greenhouse gas concentrations and their extensions from 1765 to 2300. *Climatic Change*, **109**, 213–241, doi:10.1007/s10584-011-0156-z.
- Mochizuki, T., and Coauthors, 2010: Pacific decadal oscillation hindcasts relevant to near-term climate prediction. *Proc. Natl. Acad. Sci. USA*, **107**, 1833–1837, doi:10.1073/pnas.0906531107.
- , and Coauthors, 2012: Decadal prediction using a recent series of MIROC global climate models. *J. Meteor. Soc. Japan*, **90A**, 373–383, doi:10.2151/jmsj.2012-A22.
- Msadek, R., and C. Frankignoul, 2009: Atlantic multidecadal oceanic variability and its influence on the atmosphere in a climate model. *Climate Dyn.*, **33**, 45–62, doi:10.1007/s00382-008-0452-0.
- , K. W. Dixon, T. L. Delworth, and W. Hurlin, 2010: Assessing the predictability of the Atlantic meridional overturning circulation and associated fingerprints. *Geophys. Res. Lett.*, **37**, L19608, doi:10.1029/2010GL044517.
- , C. Frankignoul, and L. Z. X. Li, 2011: Mechanisms of the atmospheric response to North Atlantic multidecadal variability: A model study. *Climate Dyn.*, **36**, 1255–1276, doi:10.1007/s00382-010-0958-0.
- , W. E. Johns, S. G. Yeager, G. Danabasoglu, T. L. Delworth, and A. Rosati, 2013: The Atlantic meridional heat transport at 26.5°N and its relationship with the MOC in the RAPID array and the GFDL and NCAR coupled models. *J. Climate*, **26**, 4335–4356, doi:10.1175/JCLI-D-12-00081.1.
- Murphy, A. H., 1988: Skill scores based on the mean-square-error and their relationships to the correlation coefficient. *Mon. Wea. Rev.*, **116**, 2417–2424, doi:10.1175/1520-0493(1988)116<2417:SSBOTM>2.0.CO;2.
- Reverdin, G., 2010: North Atlantic Subpolar Gyre surface variability (1895–2009). *J. Climate*, **23**, 4571–4584, doi:10.1175/2010JCLI3493.1.
- Robson, J. I., 2010: Understanding the performance of a decadal prediction system. Ph.D. thesis, University of Reading, 244 pp. [Available online at http://www.met.reading.ac.uk/~swr06jir/thesis/JIR_thesis.pdf.]
- , R. T. Sutton, K. Lohmann, D. M. Smith, and M. D. Palmer, 2012a: Causes of the rapid warming of the North Atlantic Ocean in the mid-1990s. *J. Climate*, **25**, 4116–4134, doi:10.1175/JCLI-D-11-00443.1.
- , —, and D. M. Smith, 2012b: Initialized decadal predictions of the rapid warming of the North Atlantic Ocean in the mid 1990s. *Geophys. Res. Lett.*, **39**, L19713, doi:10.1029/2012GL053370.
- , —, and —, 2013: Predictable climate impacts of the decadal changes in the ocean in the 1990s. *J. Climate*, **26**, 6329–6339, doi:10.1175/JCLI-D-12-00827.1.
- Roemmich, D., and J. Gilson, 2009: The 2004–2008 mean and annual cycle of temperature, salinity, and steric height in the global ocean from the Argo Program. *Prog. Oceanogr.*, **82**, 81–100, doi:10.1016/j.pocean.2009.03.004.
- Sarafanov, A., A. Falina, A. Sokov, and A. Demidov, 2008: Intense warming and salinification of intermediate waters of southern origin in the eastern subpolar North Atlantic in the 1990s to mid-2000s. *J. Geophys. Res.*, **113**, C12022, doi:10.1029/2008JC004975.
- Sévellec, F., and A. V. Fedorov, 2013: The leading, interdecadal eigenmode of the Atlantic meridional overturning circulation in a realistic ocean model. *J. Climate*, **26**, 2160–2183, doi:10.1175/JCLI-D-11-00023.1.
- Smith, D. M., S. Cusack, A. W. Colman, C. K. Folland, G. R. Harris, and J. M. Murphy, 2007: Improved surface temperature prediction for the coming decade from a global climate model. *Science*, **317**, 796–799, doi:10.1126/science.1139540.
- , R. Eade, N. Dunstone, D. Fereday, J. M. Murphy, H. Pohlmann, and A. Scaife, 2010: Skillful multi-year predictions of Atlantic hurricane frequency. *Nat. Geosci.*, **3**, 846–849, doi:10.1038/ngeo1004.
- , —, and H. Pohlmann, 2013: A comparison of full-field and anomaly initialization for seasonal to decadal climate prediction. *Climate Dyn.*, **41**, 3325–3338, doi:10.1007/s00382-013-1683-2.
- Stock, C. A., and Coauthors, 2011: On the use of IPCC-class models to assess the impact of climate on living marine resources. *Prog. Oceanogr.*, **88**, 1–27, doi:10.1016/j.pocean.2010.09.001.
- Stockdale, T. N., 1997: Coupled ocean–atmosphere forecasts in the presence of climate drift. *Mon. Wea. Rev.*, **125**, 809–818, doi:10.1175/1520-0493(1997)125<0809:COAFIT>2.0.CO;2.
- Sutton, R. T., and D. L. R. Hodson, 2005: Atlantic Ocean forcing of North American and European summer climate. *Science*, **309**, 115–118, doi:10.1126/science.1109496.

- Taylor, K. E., R. J. Stouffer, and G. A. Meehl, 2012: An overview of CMIP5 and the experiment design. *Bull. Amer. Meteor. Soc.*, **93**, 485–498, doi:10.1175/BAMS-D-11-00094.1.
- Terray, L., 2012: Evidence for multiple drivers of North Atlantic multi-decadal climate variability. *Geophys. Res. Lett.*, **39**, L19712, doi:10.1029/2012GL053046.
- Ting, M., Y. Kushnir, R. Seager, and C. Li, 2009: Forced and internal twentieth-century SST trends in the North Atlantic. *J. Climate*, **22**, 1469–1481, doi:10.1175/2008JCLI2561.1.
- van Oldenborgh, G. J., F. J. Doblas-Reyes, B. Wouters, and W. Hazeleger, 2012: Decadal prediction skill in a multi-model ensemble. *Climate Dyn.*, **38**, 1263–1280, doi:10.1007/s00382-012-1313-4.
- Vecchi, G. A., and Coauthors, 2013: Multiyear predictions of North Atlantic hurricane frequency: Promise and limitations. *J. Climate*, **26**, 5337–5357, doi:10.1175/JCLI-D-12-00464.1.
- Visbeck, M., E. P. Chassignet, R. G. Curry, T. L. Delworth, R. R. Dickson, and G. Krahnmann, 2003: The ocean's response to North Atlantic Oscillation variability. *The North Atlantic Oscillation: Climatic Significance and Environmental Impact*, *Geophys. Monogr.*, Vol. 134, Amer. Geophys. Union, 113–145.
- von Storch, H., and F. W. Zwiers, 1999: *Statistical Analysis in Climate Research*. Cambridge University Press, 484 pp.
- Williams, R. G., V. Roussenov, D. M. Smith, and M. S. Lozier, 2014: Decadal evolution of ocean thermal anomalies in the North Atlantic: The effects of Ekman, overturning, and horizontal transport. *J. Climate*, **27**, 698–719, doi:10.1175/JCLI-D-12-00234.1.
- Wouters, B., W. Hazeleger, S. Drijfhout, G. J. van Oldenborgh, and V. Guemas, 2013: Multiyear predictability of the North Atlantic subpolar gyre. *Geophys. Res. Lett.*, **40**, 3080–3084, doi:10.1002/grl.50585.
- Yang, X., and Coauthors, 2013: A predictable AMO-like pattern in the GFDL fully coupled ensemble initialization and decadal forecasting system. *J. Climate*, **26**, 650–661, doi:10.1175/JCLI-D-12-00231.1.
- Yashayaev, I., 2007: Hydrographic changes in the Labrador Sea, 1960–2005. *Prog. Oceanogr.*, **73**, 242–276, doi:10.1016/j.pocean.2007.04.015.
- Yeager, S. G., A. Karspeck, G. Danabasoglu, J. Tribbia, and H. Teng, 2012: A decadal prediction case study: Late twentieth-century North Atlantic Ocean heat content. *J. Climate*, **25**, 5173–5189, doi:10.1175/JCLI-D-11-00595.1.
- Zhang, R., 2010: Latitudinal dependence of Atlantic meridional overturning circulation (AMOC) variations. *Geophys. Res. Lett.*, **37**, L16703, doi:10.1029/2010GL044474.
- , and T. L. Delworth, 2006: Impact of Atlantic multidecadal oscillations on India/Sahel rainfall and Atlantic hurricanes. *Geophys. Res. Lett.*, **33**, L17712, doi:10.1029/2006GL026267.
- Zhang, S., M. J. Harrison, A. Rosati, and A. T. Wittenberg, 2007: System design and evaluation of coupled ensemble data assimilation for global oceanic climate studies. *Mon. Wea. Rev.*, **135**, 3541–3564, doi:10.1175/MWR3466.1.